THE HALL COEFFICIENT OF INDIUM IN THIN EVAPORATED FILMS

THOMAS EDWARD DYER
and
GEORGE TSANTES, JR.

THE HALL COEFFICIENT OF INDIUM

IN THIN EVAPORATED FILMS

by

Thomas Edward Dyer
Lieutenant Commander, United States Navy
B.S., Naval Academy, 1957

and

George Tsantes, Jr.
Lieutenant Commander, United States Navy
B.S., Naval Academy, 1955

Submitted in partial fulfillment of the
requirements for the degree of

MASTER OF SCIENCE IN PHYSICS

from the

NAVAL POSTGRADUATE SCHOOL
December 1967

ABSTRACT

The Hall coefficient has been measured at liquid helium temperatures in the magnetic field range of 0.08-3.8 kilogauss for evaporated indium films with thicknesses between 900 and 2,500 Angstroms. For all films studied the Hall coefficient was positive; there was no sign reversal of the type observed in some rolled films at low magnetic fields. The coefficients obtained were slightly smaller than those previously reported for bulk films at comparable values of reduced magnetic field. Below the superconducting critical temperature in the weak-field region a large and unexpected transverse potential difference, independent of magnetic field direction, was observed. As the magnetic field was increased, this potential difference reversed sign and underwent damped, aperiodic oscillations in some samples. However, in the higher-field region a normal Hall voltage was present, and the Hall coefficient was in good agreement with the data above the critical temperature.

DUDLEY KNOX LIBRARY
NAVAL POSTGRADUATE SCHOOL
MONTEREY CA 93943-5101

TABLE OF CONTENTS

LIST OF TABLES

LIST OF ILLUSTRATIONS

ACKNOWLEDGEMENTS

The authors greatly appreciate the guidance, encouragement, and assistance given them by Professor J. N. Cooper of the Naval Postgraduate School, and for the outstanding technical assistance and efforts of Mr. R. A. Garcia of the Naval Postgraduate School.

1. Introduction.

When a conductor carrying an electric or thermal current is placed in a magnetic field, a wide range of galvanomagnetic and thermomagnetic effects result. The first of the galvanomagnetic effects, discovered in 1879, is known as the Hall effect [1]. For an understanding of the Hall effect, consider a metallic conductor in the form of a thin rectangular sample (Fig. 1) placed in a magnetic field $\underline{B}_z$ perpendicular to the electric current density $\underline{J}_x$. The force on a charge moving in a magnetic field is given by the Lorentz force equation

$$\overline{F} = q\,\overline{v} \times \overline{B} \tag{1}$$

where $\underline{q}$ is the charge and $\overline{v}$ its velocity. If the current is carried by free electrons moving in the $-\underline{x}$ direction, the charge carriers are deflected in the $-\underline{y}$ direction by the magnetic field. As a consequence, electrons accumulate on one face of the specimen, and a positive ion excess is established on the opposite face. This creates a transverse electric field, known as the Hall field, which is perpendicular to both the current density and magnetic field. On the average, this Hall field $\underline{E}_y$ just compensates the force due to the magnetic field. The Hall coefficient (Hall constant) $\underline{R}_H$ is defined as

$$R_H \equiv \frac{E_y}{J_x B_z} \tag{2}$$

In the laboratory one ordinarily measures the potential difference $\underline{V}_y$ developed across the width $\underline{w}$ of the specimen. To express the Hall coefficient in terms of the Hall voltage $\underline{V}_y$ and the current $\underline{I}_x$ through the specimen, we utilize

$$V_y = E_y\, w \qquad \text{and} \qquad I_x = J_x\, wt \tag{3a,b}$$

where $\underline{t}$ is the specimen thickness, to obtain

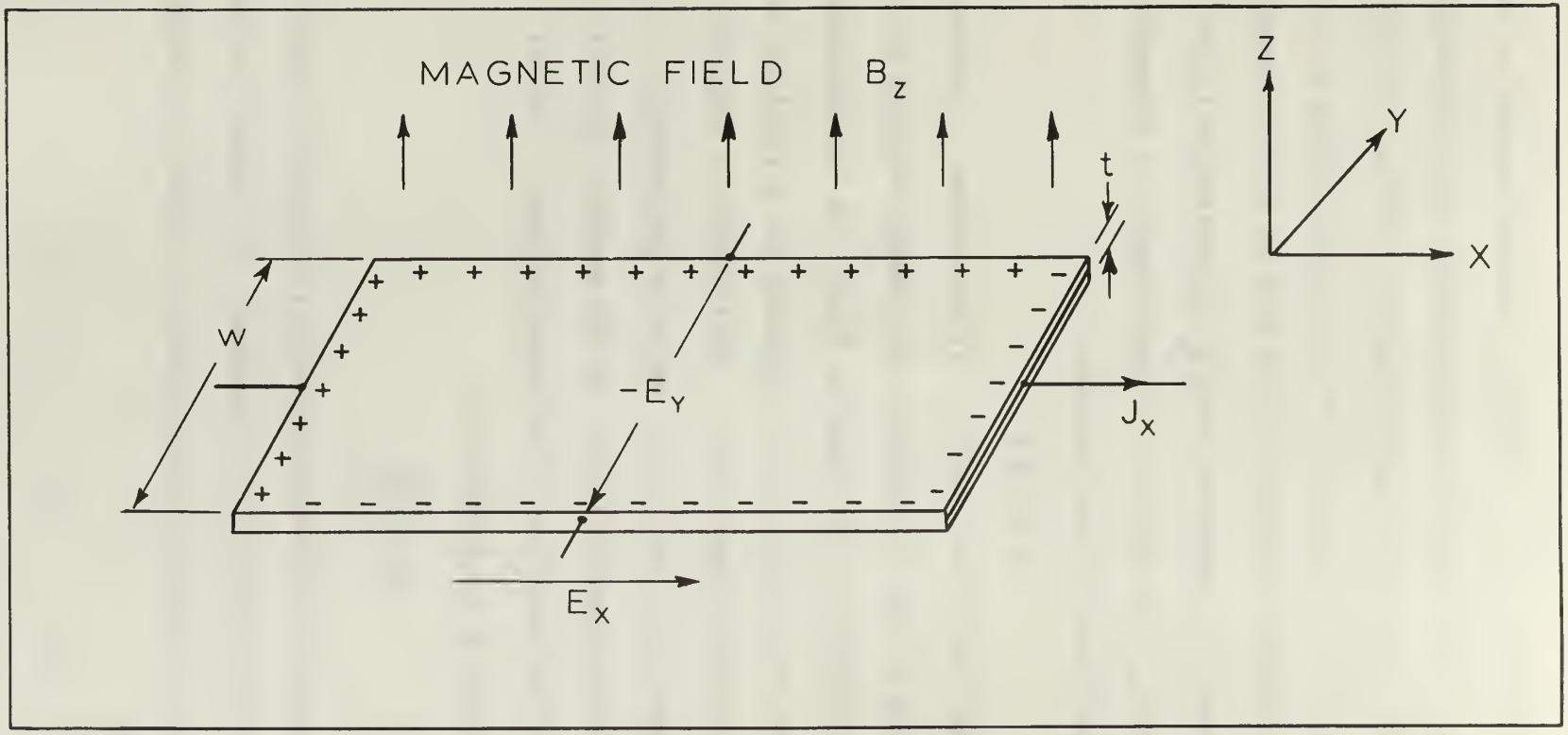

Figure 1. The standard geometry for the Hall effect in a rectangular specimen with negative carriers. For positive carriers E_y is reversed.

$$R_H = \frac{V_y/w}{J_x B_z} \cdot \frac{t}{t} = \frac{V_y t}{I_x B_z} \tag{4}$$

Looking once again at the force produced by the motion of a charge in a magnetic field, we observe that the velocity $\bar{v}$ in the Lorentz force equation is the instantaneous velocity of the charge. Electrons moving through a conductor experience a succession of accelerations and decelerations, but they acquire a certain average velocity, or drift velocity $\bar{v}_D$, where $\bar{v}_D$ may be as small as $|\bar{v}| \times 10^{-9}$. Since $\bar{v}_D$ is the average velocity, the average force produced by this motion of the charges in the magnetic field is $q\bar{v}_D \times \bar{B}$ which is just compensated by the force of the electric Hall field,

$$-q v_D B_z + q E_y = 0 \tag{5}$$

(Throughout the present discussion, MKS units are used in equations.) When there is a single kind of charge carrier, the current density is given by

$$J_x = nq v_D \tag{6}$$

where n is the carrier concentration. Substituting v_D from Eq. 6 into Eq. 5 yields

$$\frac{J_x}{n} B_z = q E_y$$

or

$$\frac{E_y}{J_x B_z} = \frac{1}{nq} \tag{7}$$

By comparing Eqs. 7 and 2 it is readily seen that

$$R_H = \frac{1}{nq} \tag{8}$$

Thus, for free-electron carriers, the Hall coefficient is negative.

The study of the Hall effect in indium is of particular interest for it exhibits behavior quite different from the free-electron predictions

outlined above. At 77°K and at 4.2°K the Hall coefficient of bulk indium is positive, opposite in sign to that predicted for electrons, although R_H is negative at room temperature. That the Hall coefficient may change sign when there are two (or more) groups of charge carriers is well known from studies on semiconductors.

For monovalent elements the Hall coefficient based on the free-electron model is in reasonably good agreement with the observed values. However, for most bivalent elements the Hall coefficient is positive and opposite to that predicted for free electrons. To improve on the predictions of the free-electron model, a two-band model is sometimes used to explain the galvanomagnetic effects. This model assumes two separate groups of carriers; that is, electrons or holes in more than one band take part in conduction at the same time. Based on electron conduction and hole conduction in adjacent bands, the two-band model Hall coefficient may be calculated to be [2]

$$R_H = -\frac{1}{e}\frac{\frac{\sigma_e^2}{n_e} - \frac{\sigma_h^2}{n_h}}{(\sigma_e + \sigma_h)^2} \tag{9}$$

where e is the magnitude of the electron charge, n_e and n_h are the electron and hole concentrations respectively, and σ_e and σ_h are the electron and hole conductivities respectively. Utilizing the relationships

$$\sigma = \frac{ne^2\tau}{m^*} \quad \text{and} \quad \mu = \frac{e\tau}{m^*} \tag{10 a,b}$$

where τ is the collision time or relaxation time, m^* the effective mass, and μ the mobility of the carriers, Eq. 9 can be rewritten as

$$R_H = -\frac{1}{e}\frac{n_e\mu_e^2 - n_h\mu_h^2}{(n_e\mu_e + n_h\mu_h)^2} \tag{11}$$

From Eqs. 9 or 11 we see that the Hall coefficient is a difference between two terms. R_H may be positive or negative and if the terms are almost equal then quite small changes in the carrier mobilities or concentrations may influence the Hall constant drastically.

Experimental results on the behavior of the Hall coefficient of indium are not very numerous. In 1950 Borovik [3] conducted Hall effect experiments on a polycrystalline plate of indium. The plate thickness measured 0.104 mm and data were obtained at 4.2°K, 14.2°K, 20.4°K and 78°K. The Hall coefficient was independent of the field only at the liquid nitrogen temperature. At the lower temperatures the Hall coefficient increased with the magnetic field, and the rate of change increased with decreasing temperature. In the low-field region and at a temperature of 4.2°K a sign reversal of the Hall coefficient was observed. In 1959 Borovik and Volotskaya [4] investigated galvanomagnetic phenomena on a single crystal indium specimen, 1.84 mm in diameter and 12.55 mm between potential leads. Measurements at 4.2°K resulted in a positive Hall constant ($R_H = 1.5 \times 10^{-10}$ meter^3/ampere-sec) which was independent of magnetic field strength. Further investigation of the Hall effect in indium plates was conducted in 1965 by Cooper, Cotti, and Rasmussen [5], who corroborated the findings of Borovik concerning the change of sign of the Hall coefficient with magnetic field for very thin (0.013 mm and 0.025 mm) films, but not for ones with thickness greater than 0.08 mm. This phenomenon was observed in samples in the low-field region at 4.2°K and 3.5°K. The data on Hall coefficient magnitude versus magnetic field strength were generally in good agreement with the Borovik results except for the sign. In 1966 van der Mark, Olsen, and Rasmussen [6] reported a positive Hall coefficient of indium at 4.2°K, but the addition

of as little as 10^{-2}% of lead or gallium changes its sign. The rate of change of the Hall coefficient with impurity concentration decreases as the impurity content is increased.

The previous Hall coefficient investigations of indium films were limited to plates, varying in thickness from 0.013 to 0.63 mm, which were pressed (or rolled) from very pure bulk material. The present study of the Hall coefficient of indium is restricted to evaporated films. The advantage of utilizing evaporated films is that the film thickness can be significantly reduced compared to that of films rolled or pressed from bulk indium. However, with respect to bulk films, evaporated ones have the inherent disadvantage of a large reduction in purity.

The primary purpose of this investigation was to gather data concerning the behavior of the Hall coefficient of indium in thin evaporated films. Of special interest in the investigation was the phenomenon of a possible sign reversal of the Hall coefficient as the magnetic field is varied. A further objective of this investigation was the possible verification of the theoretical prediction of Sondheimer [7] that the Hall coefficient of a thin film, in the low-field limit, increases with decreasing film thickness. Based on the assumption that conduction electrons may be treated as if they were free, Sondheimer calculated the resistivity and the Hall coefficient of a thin film with a magnetic field normal to its surface. In addition to the low-field prediction, his calculations showed that for higher fields the Hall coefficient should have weak oscillations around the bulk value.

2. Experimental Equipment.

The experimental equipment necessary to satisfactorily control and monitor the environment of the specimen under test, and to obtain measurements of the various parameters of interest, was composed of a cryogenic system (Fig. 2), an electrical system (Fig. 3), and the test specimen (Fig. 4).

The cryogenic system (Fig. 2) was composed of two Dewar flasks, concentrically positioned, and suspended from a shelf by support collars. The volume between the double walls of the inner Dewar was evacuated, filled with 500 microns of nitrogen gas, and then sealed. This nitrogen gas condensed when the inner Dewar was filled with liquid helium, with the resulting vacuum providing insulation for the helium bath contained in the Dewar. This helium Dewar was sealed by the test assembly, consisting of a round plate with an attached 30-inch long, hollow stainless steel tube which extended to the lower end of the Dewar. Electrical connection terminals for power and instrumentation were provided on top of this plate. Leads passed from the bottom of this plate, through the hollow tube, to terminals on a connection board mounted on the tube's lower end. The specimen and its holder were attached to this board, with the specimen leads connected to the terminals. The support collar assembly for the inner Dewar was provided with ports to which the pressure regulating and measuring equipment was connected. The pressure, and hence temperature, of the helium bath was maintained constant by a Crittenden regulating valve. Operation of this valve and pressure measurement was as described by Lauer and Nunneley [8], subject to the control modification of Eckert and Donnelly [9]. Since the temperature of the helium bath was an extremely sensitive parameter once the superconducting

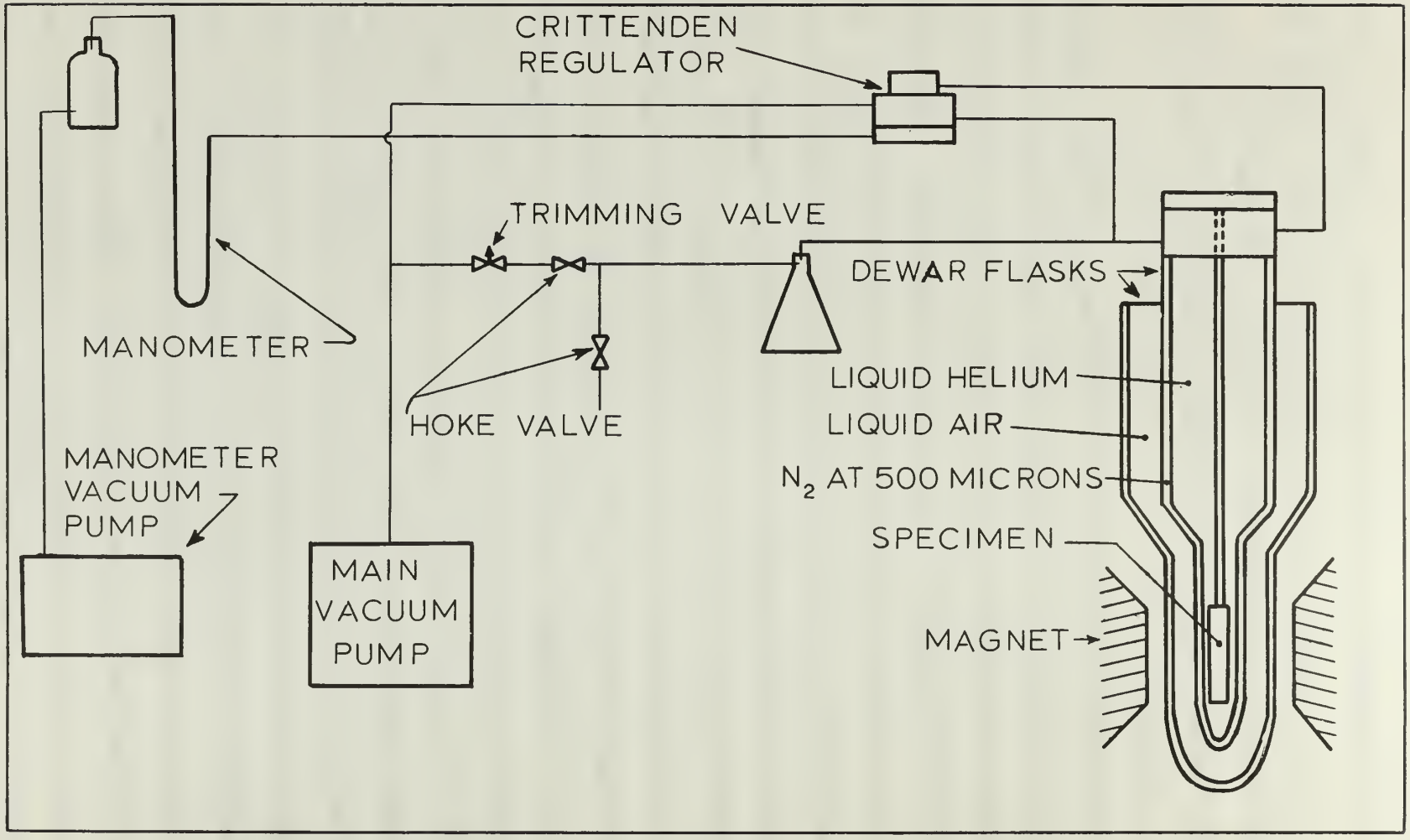

Figure 2. Schematic diagram of cryogenic system for Hall effect experiment.

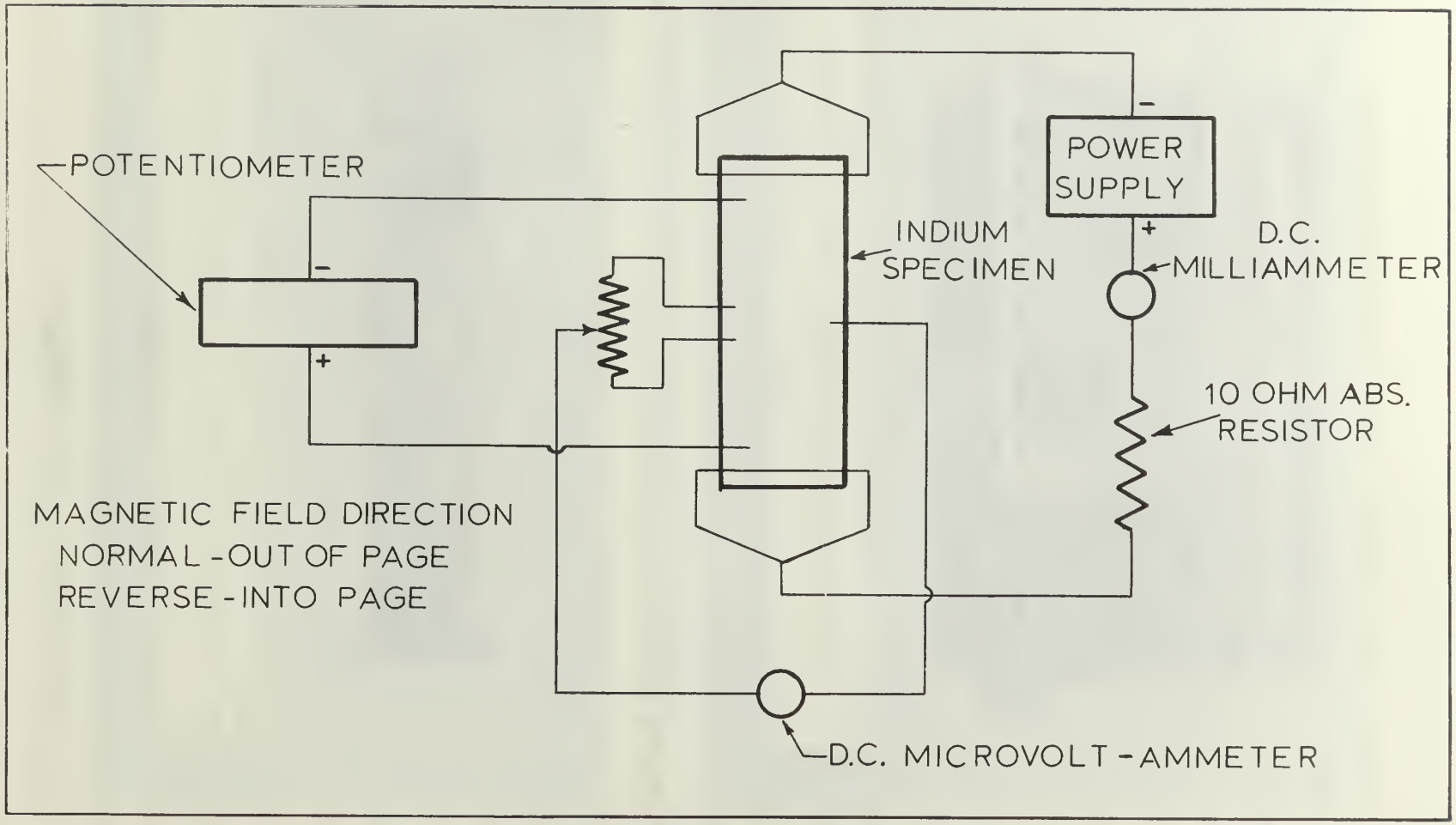

Figure 3. Schematic diagram of electrical system for Hall effect measurements.

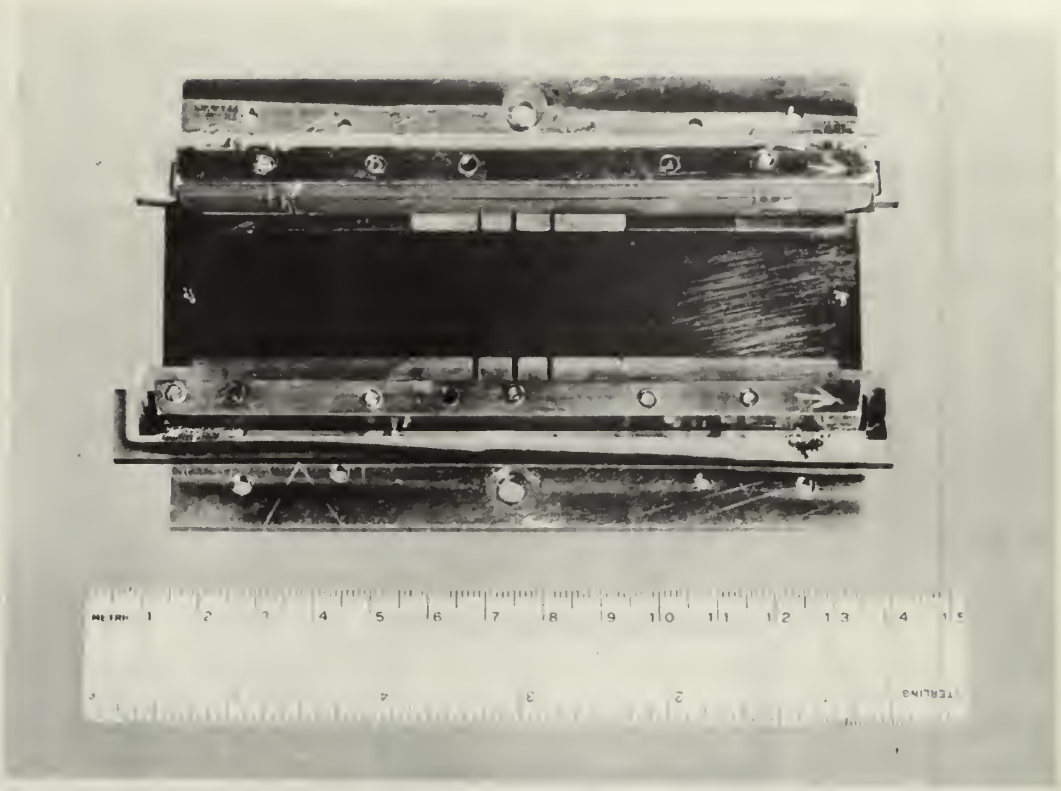

Figure 4(a). Specimen mounted in specimen preparation holder showing razor-blade mask.

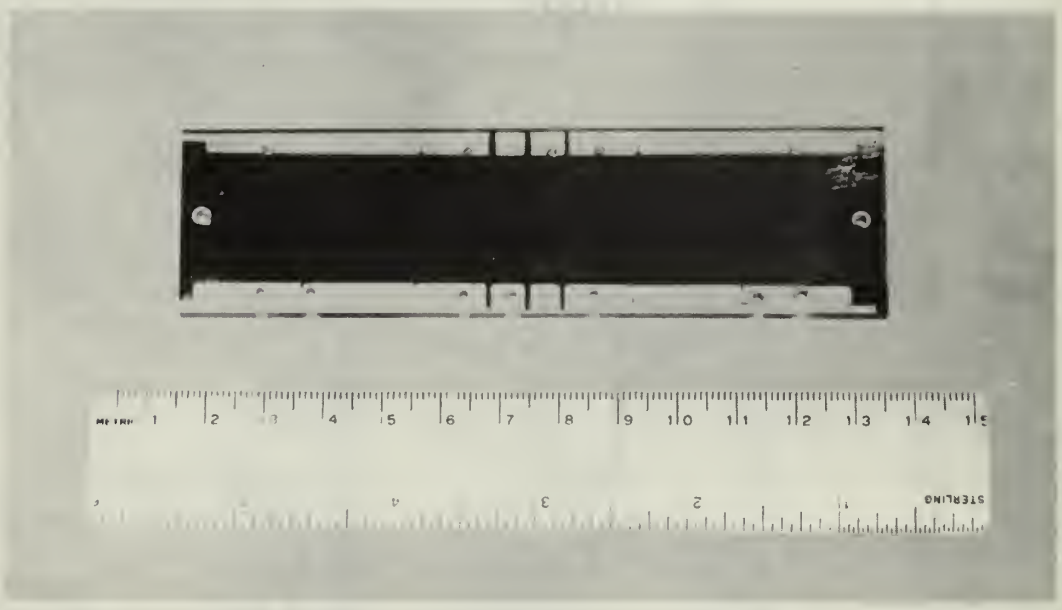

Figure 4(b). Indium specimen.

region had been entered, an additional valve, in series with the Hoke valve and large vacuum pump, served as a trimming valve to provide finer pressure control. The vacuum pumps utilized in this system were a 30.4 ft^3/min Kinney forepump (Kinney Manufacturing Division, The New York Air Brake Company, Boston, Massachusetts, Model KD 30) for the main pump, and a Duo-Seal Vacuum Pump (W. M. Welch Manufacturing Company, Chicago, Illinois) for the manometer pump. The outer Dewar was kept filled with liquid nitrogen to minimize external heat transfer to the helium bath in the inner Dewar. A relief valve was provided on the test stand to prevent build-up of excessive pressure within the inner Dewar.

The magnetic field was provided by a Model V-4007 six-inch, water-cooled, electromagnet and a Model V-2200 Regulated Magnet Power Supply, both made by Varian Associates, Palo Alto, California. The magnet was positioned so that the specimen, when suspended into the Dewar flasks on the test assembly, was centered between the pole faces of the magnet. A gap spacing of 3.75 inches, with the standard 6-inch diameter cylindrical pole caps installed, was needed to permit 180^{o} rotation of the magnet (for field reversal) without damaging the outer cryostat. (A field kit was subsequently obtained from Varian which accomplished field reversal electrically rather than mechanically through magnet rotation.) With the gap spacing of 3.75 inches, a variable field from 0.08 to 3.8 kilogauss was available.

The electrical system (Fig. 3) consisted of power supply and measuring circuits. The current through the specimen was provided by a Transistorized Power Supply (Power Designs Pacific, Palo Alto, California, Model 2015R) operated in the "Constant Current" mode. To minimize load variations on the power supply, although technically unnecessary, a

10-ohm absolute, precision resistor (Leeds and Northrup Company, Philadelphia, Pennsylvania) was placed in series with the specimen. A dc milliammeter (Weston Electrical Instrument Corporation, Newark, New Jersey, Model 931) was used to measure current to the specimen. The measurement of voltage drop over the length of the film was made using a precision potentiometer (Minneapolis-Honeywell Regulator Company, Rubicon Instruments, Philadelphia, Pennsylvania, Model 2733). To measure the Hall voltage developed across the width of the specimen, two leads which were connected to the same side of the film, but with a separation of 12 mm, were attached across a 50-ohm, variable tap, oil-immersed resistor (International Resistance Company, St. Petersburg Division, St. Petersburg, Florida, Type H 755 CT - 5423). The potential of the variable tap (Fig. 3) with respect to a lead connected to the opposite side of the film was measured using a dc microvolt-ammeter (Hewlett-Packard Company, Palo Alto, California, Model 425A).

As a result of silvering of the two cryostats, visual determination of helium level in the inner cryostat was difficult. Therefore, two 150-ohm resistors were mounted on the tube of the test assembly. Their resistance, which changed markedly upon immersion in liquid helium, was measured using a volt-ohm-milliammeter (Simpson Electric Company, Chicago, Illinois, Model 267). This rather basic circuit provided "positive" indication as to whether or not the resistors were covered by liquid helium.

The test specimens (Fig. 4) were all thin, evaporated films of indium, with thicknesses ranging from 900 to 2500 Angstroms. These films, deposited on plexiglas substrates, had an active length, measured between the power connections, of 10 cm, and a width of 2.4 cm. Provision for

measuring voltage drop over the film's length was provided by two connections spaced 8.5 cm apart along one edge of the film. Connections for measuring the Hall voltage developed across the film's width were provided by legs of film extending out from both sides of the main film and positioned midway between the power connections (Fig. 4). Equipment and methods used in film preparation are described in Appendix I; the choice of substrate material and the connections to the film are discussed in Appendix II.

3. Experimental Procedure.

Following sample preparation (Appendix I) and a continuity check, sample and holder were bolted together, attached to the test assembly, and continuity re-checked. The test assembly was then bolted into place on the test stand, and the sample inserted into the inner cryostat so that its surface was centered between and parallel to the pole faces of the electromagnet. Positioned thusly, the film was perpendicular to the magnetic field. After connecting the external wiring to the terminals on the top plate of the test assembly, a small current (40 mamp or less) was passed through the sample; the potential drop across the sample and the ambient temperature were then recorded. This was done rapidly and repeatedly, the current flow being interrupted between measurements to minimize the effects of resistive heating.

After these data were obtained, the Hall voltage measuring circuit was checked out to insure that the circuit could be satisfactorily nulled with no magnetic field applied. This circuit, which is shown schematically in Fig. 3, employed a precision variable resistor connected as a voltage divider between two leads from one side of the film. The lead from the sliding contact of this voltage divider and a single lead from the opposite side of the film were connected to the dc microvolt-ammeter. This meter was operated in a mode that permitted the accurate measurement of a potential difference between two leads, neither one of which was necessarily at ground potential. Additionally, the meter and its probe were factory calibrated as a unit such that for copper wiring, as used throughout the circuit, with clamped rather than soldered connections, and contact with the film utilizing the legs and method described in Appendix II, no corrections to meter readings for bi-metallic contact

potentials were required. Thus, with current flowing through the specimen, the meter could be used as a galvanometer and a "null" or zero deflection point found by adjusting the voltage divider.

After completion of room temperature readings and a satisfactory null of the Hall voltage circuit, cooldown of the specimen was started by filling the outer Dewar with liquid nitrogen. While the outer Dewar was kept filled with liquid nitrogen, the resistance of the specimen was monitored until it reached a minimum value, a process usually taking about two hours. Using a small current and again taking readings rapidly, with current interruption between readings, the potential drop across the specimen was measured, the temperature being taken as that of liquid nitrogen, $77^{o}K$. The Hall voltage circuit was again checked out for a satisfactory null.

From the data obtained at room temperature and at liquid nitrogen temperature, resistance values for the standard ambient temperature, $20^{o}C(293^{o}K)$, and the Debye temperature, $100^{o}K$, were computed by linear interpolation. These resistances were designated as $\underline{R}_{293}$ and $\underline{R}_{\theta}$ respectively.

After these preliminary steps had been satisfactorily carried out, the transfer of liquid helium into the inner Dewar was commenced. The accumulation of liquid helium in the inner Dewar was monitored by the level-detecting circuit until indication that the lower monitoring resistor was covered was shown by its greatly increased resistance. The level could then be monitored visually, and a sufficient amount of liquid helium was added to ensure that the specimen would remain covered during the entire experiment.

The current through the specimen was adjusted to the desired value,

generally 1000 mamp, the pressure was stabilized and determined from the manometer, and the Hall circuit nulled. Once these steps were completed, the magnetic field was turned on at its minimum value. The magnetic field was raised in steps until a reading was obtained on the Hall circuit. No adjustments of the resistor were made after turning on the field. Thus, readings obtained were those caused by the magnetic field or associated with a zero-drift. The Hall voltage, the magnet current, and the potential drop along the specimen in the direction of current flow were recorded. The magnetic field was increased in steps to a maximum and then decreased in steps back to its minimum value. Data were recorded for each field setting. Upon satisfactory completion of a data run, the magnetic field direction was reversed to check for consistency of measurements over the entire field range.

A curve of magnetic field vs magnet current for a gap width of 3.75" was constructed by linear interpolation between the field data for 2" and 4" gap widths supplied by the manufacturer. From this prepared curve, the field at each data point was computed. No corrections for hysteresis loss were made in the raw data.

The initial data run for each specimen was conducted at atmospheric pressure. For subsequent data runs, the pressure (and hence temperature of the specimen) was decreased to a convenient value and another set of measurements made. Nulling of the Hall circuit was accomplished with no field for each set of data until, when the sample specimen became superconducting, normal nulling was no longer possible. However, as the null shifted only slightly with temperature, the careful nulling of the circuit on the preceding data runs ensured that the circuit was essentially nulled for all other data runs. However, since the exact position of

the null could not be determined, a full set of data was required for the normal and reversed field directions. With this dual set of measurements, the null setting could be accurately established.

4. Discussion of Results.

Hall effect measurements were recorded on five separate indium specimens. The designation of each specimen is shown in Table 1, and the specimen thicknesses which varied from 900 to 2500 Angstroms are also listed. For each data run, which was conducted at a constant temperature, the following readings were recorded: Hall voltage $\underline{V}_y$; magnet current $\underline{I}_m$; electric current through specimen $\underline{I}_x$; potential drop across the specimen in the direction of current flow $\underline{V}_x$; and the magnetic field direction. Measurements on each specimen were made at several selected temperature values, the highest temperature being the boiling point of liquid helium ($4.2^{\circ}K$) and the lowest temperature being a function of the pumping capacity of the cryogenic system ($1.6^{\circ}K$).

From the potential drop $\underline{V}_x$ across the specimen at liquid helium temperature, and the corresponding electric current $\underline{I}_x$, the resistance at $4.2^{\circ}K$ $\underline{R}_F$ was directly determined. The resistances at standard ambient temperature $\underline{R}_{293}$ and at the Debye temperature $\underline{R}_{\theta}$ were determined by linear interpolation from measuring $\underline{V}_x$ at room temperature and at liquid nitrogen temperature. Utilizing the relationship

$$\frac{R_1}{R_2} = \frac{\rho_1 L}{A} \div \frac{\rho_2 L}{A} = \frac{\rho_1}{\rho_2} \tag{12}$$

where ρ is the resistivity, $\underline{L}$ and $\underline{A}$ are characteristic dimensions that are assumed to be temperature independent in this range of interest, the ratios of ρ_{293}/ρ_F and ρ_{θ}/ρ_F were computed.

The resistivity ρ is proportional to the mean free path for a one-carrier system and is a crude measure of mean free path for more complicated conductors. Table 1 also lists the ratio of dc resistivity at standard ambient temperature ρ_{293} to resistivity at $4.2^{\circ}K$ ρ_F for each

Table 1

SPECIMEN PROPERTIES and DATA RUN SETTINGS

Sample No.	Thickness t (Å)	ρ_{293}/ρ_F	Control Temperature (°K)					Current Setting (mamp)		
In-2	1200	25.0	4.2	3.44				1000	500	250
In-3	2500	38.6	4.2	3.44	2.65		1.68	1000	500	
In-4	1300	29.2	4.2	3.44	2.65		1.61	1000		
In-5	1900	36.5					1.80	1000		
In-6	900	20.9	4.2	3.44	2.65	2.02	1.79	1000		

specimen. Values of this ratio vary from a maximum of 38.6 for the thickest specimen to a minimum of 20.9 for the thinnest sample, where the behavior of the ratio was monotonic. All evaporated film specimens have much lower resistivity ratios than rolled films of bulk indium which have ratios of the order of 10^4 or higher.

The ratio of dc resistivity at the Debye temperature ρ_θ to the resistivity at 4.2°K ρ_F is utilized as a normalizing factor for the magnetic field B. The reduced resistivity ρ_F/ρ_θ when divided into the magnetic field results in a reduced magnetic field $B\rho_\theta/\rho_F$, where the resistivity at the Debye temperature becomes the reference resistivity for the metal. This correction factor is necessary in order to make comparisons between specimens with different resistivities. The magnetic field tends to make the electrons move in circular or helical orbits, and the effect of the field on the resistivity depends on the angle through which an electron is deflected between collisions. This can be measured by the variable ℓ/r where ℓ is the electronic mean free path and r is the radius of orbit. It is shown by Olsen [10] that for free electrons

$$\frac{\ell}{r} = \frac{B}{\rho} \cdot \frac{1}{nq} \tag{13}$$

or normalizing by multiplying Eq. 13 by the factor ρ_θ we have

$$\frac{\ell}{r}\ \rho_\theta = B\frac{\rho_\theta}{\rho_F} \cdot \frac{1}{nq} \tag{14}$$

This normalization to the Debye temperature resistivity permits us to compare, at a common reference, specimens with different resistivities.

During the data runs temperature control was exercised both above and below the superconducting critical temperature. At any given temperature, the transverse potential difference V_y was recorded both for

increasing and decreasing magnetic fields. The potential differences measured in the increasing field direction differed somewhat from the potential measurements for the decreasing field due to magnet hysteresis. The direction of the magnetic field was also reversed to obtain a more complete check of the Hall effect. Above the critical temperature, reversal of the field resulted in a polarity reversal of the transverse potential $\underline{V}_y$ which was consistent with the theory. Below the critical temperature reversal of the magnetic field produced a strange phenomenon. For weak fields the transverse potential $\underline{V}_y$ exhibited no change in sign with reversal of magnetic field, but further investigation showed a reversal of sign occurred when the direction of specimen current $\underline{I}_x$ was reversed. However, this abnormality disappeared in the higher-field region, and the transverse potential $\underline{V}_y$ changed sign with reversal of magnetic field direction.

In calculating Hall coefficients the magnet current readings $\underline{I}_m$ were converted to magnetic field values, and then by direct substitution of the recorded measurements into Eq. 4 ($R_H = V_y t / I_x B_z$), a Hall coefficient value $\underline{R}_H$ was obtained for each data point. However, below the critical temperature in the weak-field region where the sign of the transverse potential $\underline{V}_y$ was independent of the magnetic field direction, the values resulting from Eq. 4 are designated as pseudo Hall coefficients. Above the critical temperature and in the higher-field region below the critical temperature the behavior of the Hall coefficient was reasonable, and the results appear to be a normal Hall coefficient. For this coefficient, hysteresis introduces no serious error. Below the critical temperature the strange and unexpected values of $\underline{V}_y$ that occurred for weak fields result in a pseudo Hall coefficient, and, in this

case, the effect of hysteresis cannot be neglected. Pseudo Hall coefficient values were determined from the data measured in the increasing and decreasing field directions by a graphical averaging technique. The data were plotted for both increasing and decreasing field directions, and then an average pseudo Hall coefficient curve was determined by interpolation.

Looking now at the results in greater detail, let us first consider the data above the critical temperature. In this region 4.2°K and 3.44°K were utilized as control temperatures for the data runs. Figures 5, 6, and 7 show the Hall coefficient $\underline{R}_H$ as a function of reduced magnetic field $\underline{B}\underline{\rho}_\theta/\underline{\rho}_F$ for the In-2 (t = 1200 Å) specimen with $\underline{I}_x$ equal to 250, 500 and 1000 mamps. These curves show only slight changes in the Hall coefficient with increasing specimen current. The same conclusion can be drawn from Figs. 8 and 9, which show a plot of the Hall coefficient $\underline{R}_H$ as a function of reduced magnetic field for the In-3 (t = 2500 Å) specimen with $\underline{I}_x$ equal to 500 and 1000 mamps. On subsequent specimens data were obtained only for the specimen current $\underline{I}_x$ equal to 1000 mamps. The final two figures (10 and 11) for the data above the critical temperature show the Hall coefficient $\underline{R}_H$ as a function of reduced magnetic field for the In-4 (t = 1300 Å) specimen and the In-6 (t = 900 Å) specimen. Above the critical temperature, the Hall coefficient of these evaporated indium films was positive for all specimens throughout the magnetic field range (0.08 to 3.8 kilogauss). Moreover, the Hall coefficient $\underline{R}_H$ is virtually constant (but increasing very slowly) with magnetic field, and only small differences were observed in $\underline{R}_H$ at the two temperatures. With the exception of a single data run, the $\underline{R}_H$ values for 3.44°K either coincided with or were slightly below the $\underline{R}_H$ values for

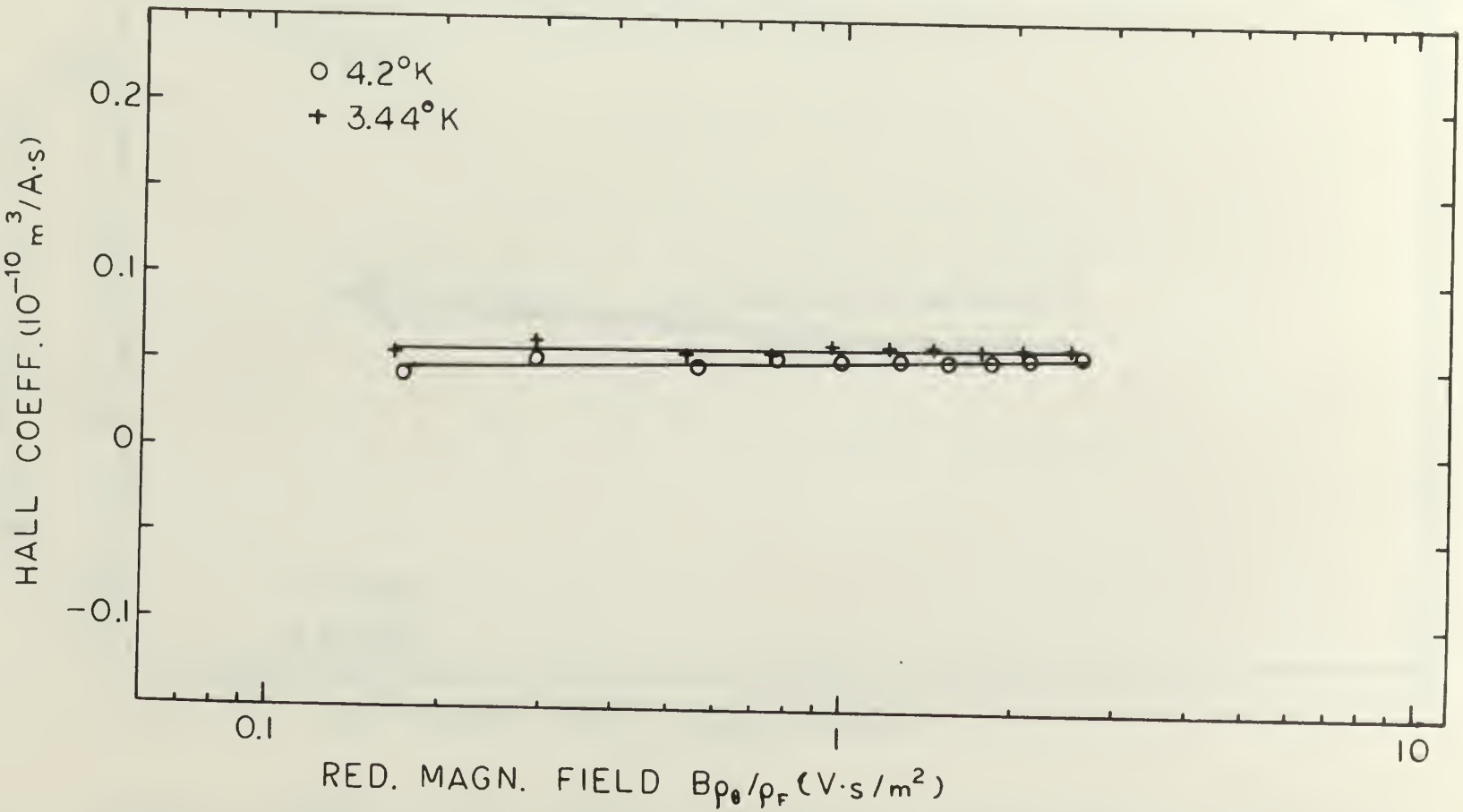

Figure 5. Dependence of Hall coefficient on magnitude of reduced magnetic field for In 2 specimen with I_x = 250 mamps.

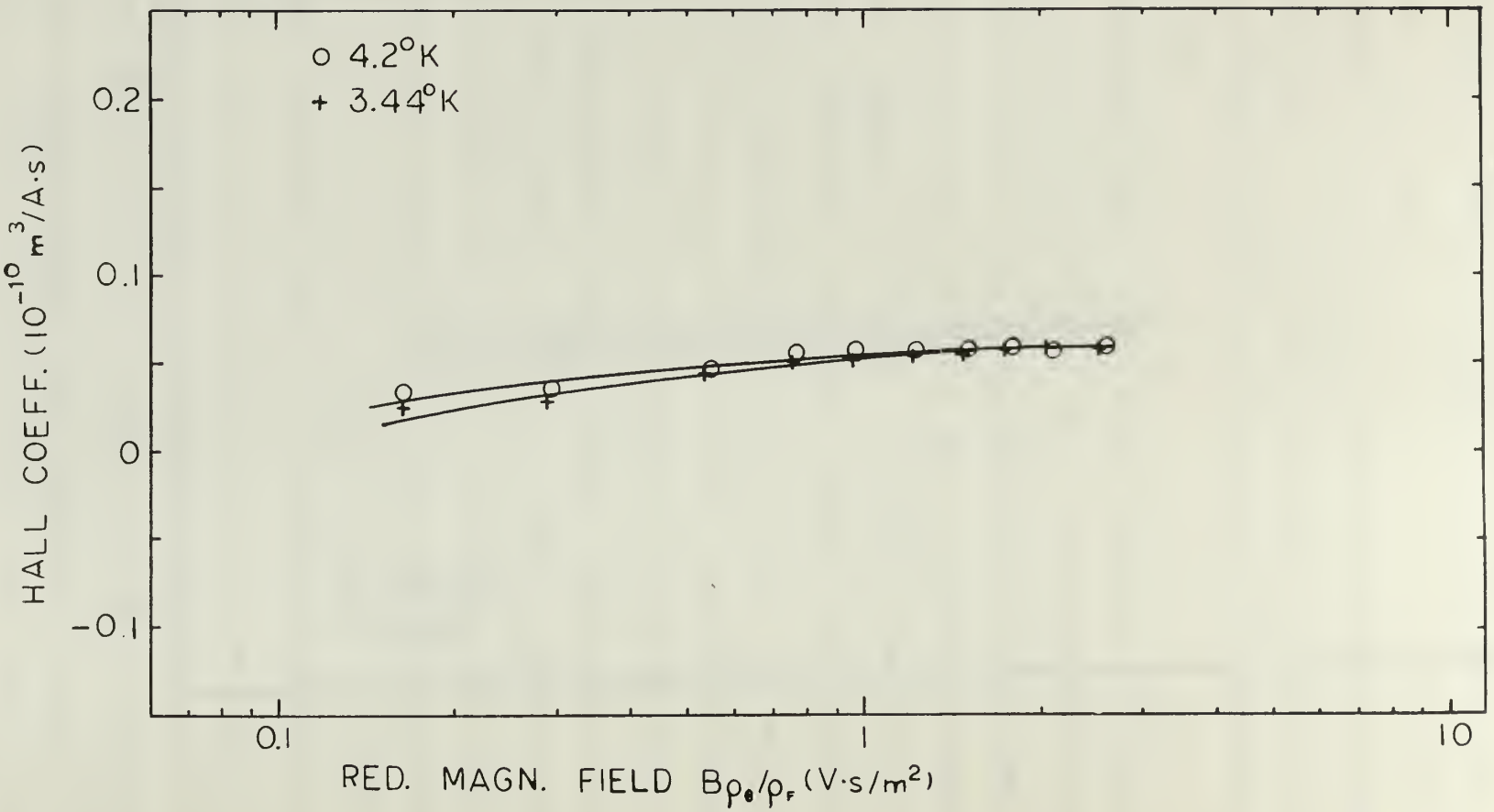

Figure 6. Dependence of Hall coefficient on magnitude of reduced magnetic field for In 2 specimen with I_x = 500 mamps.

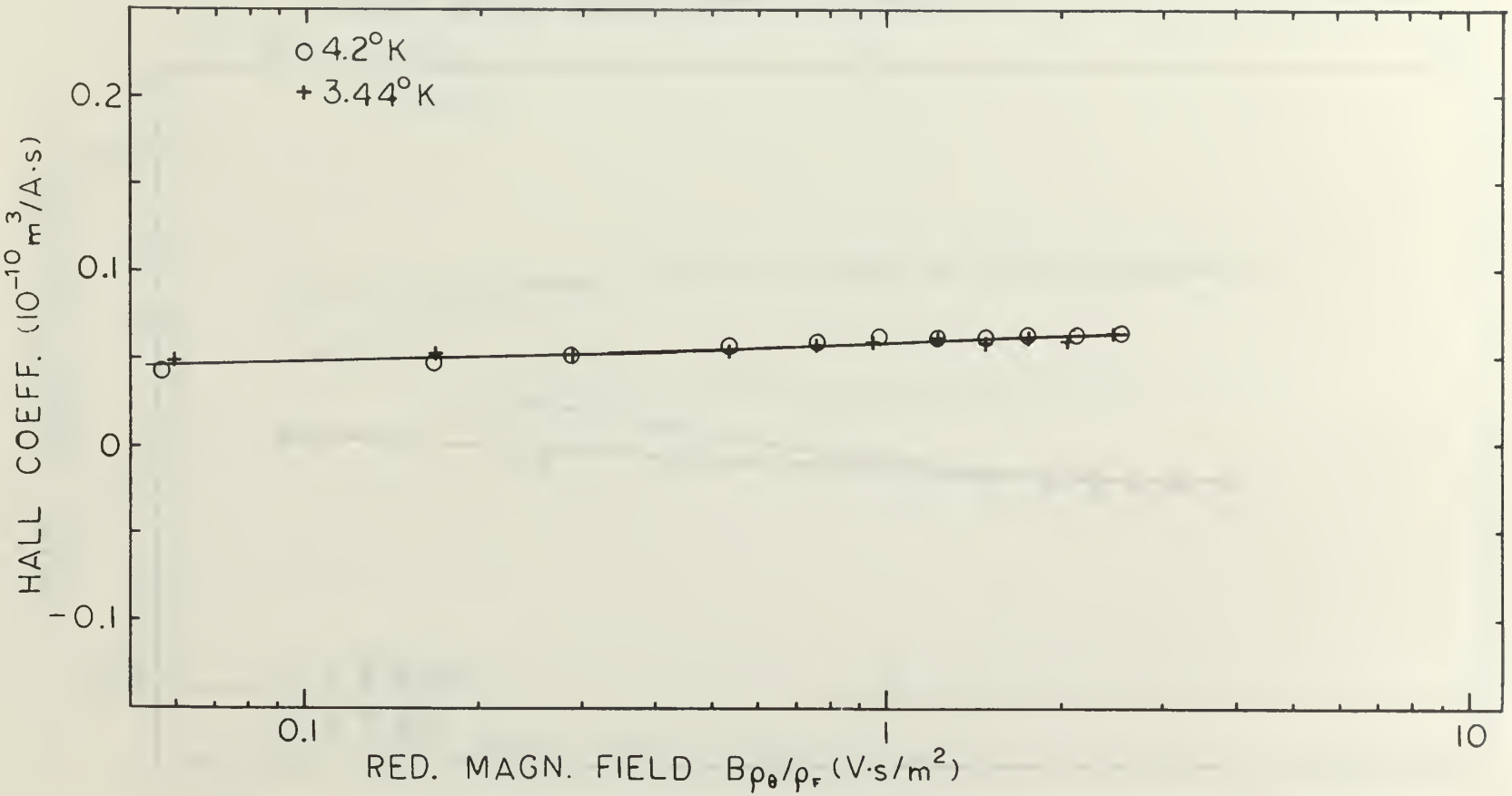

Figure 7. Dependence of Hall coefficient on magnitude of reduced magnetic field for In 2 specimen with I_x = 1000 mamps.

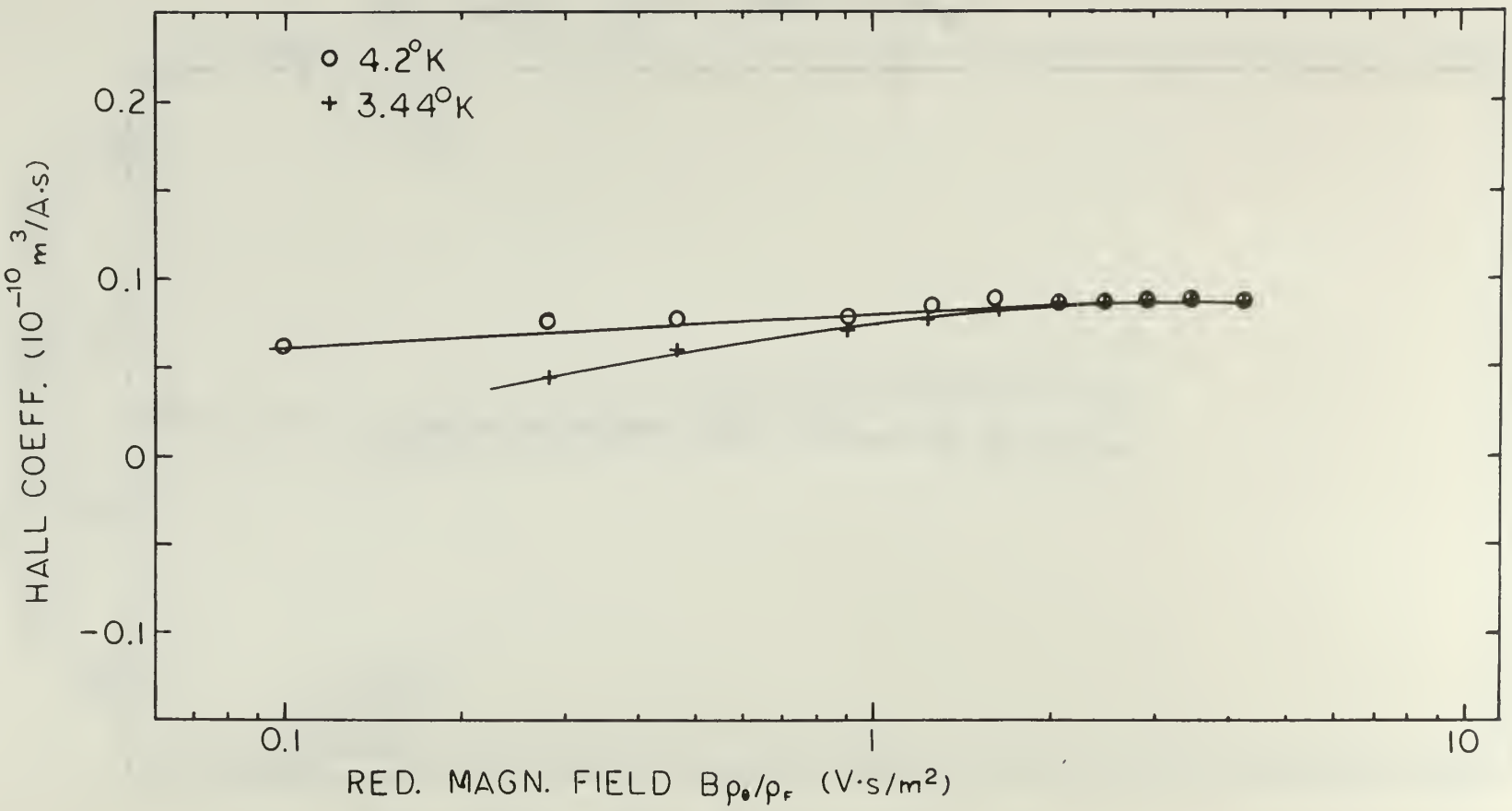

Figure 8. Dependence of Hall coefficient on magnitude of reduced magnetic field for In 3 specimen with I_x = 500 mamps.

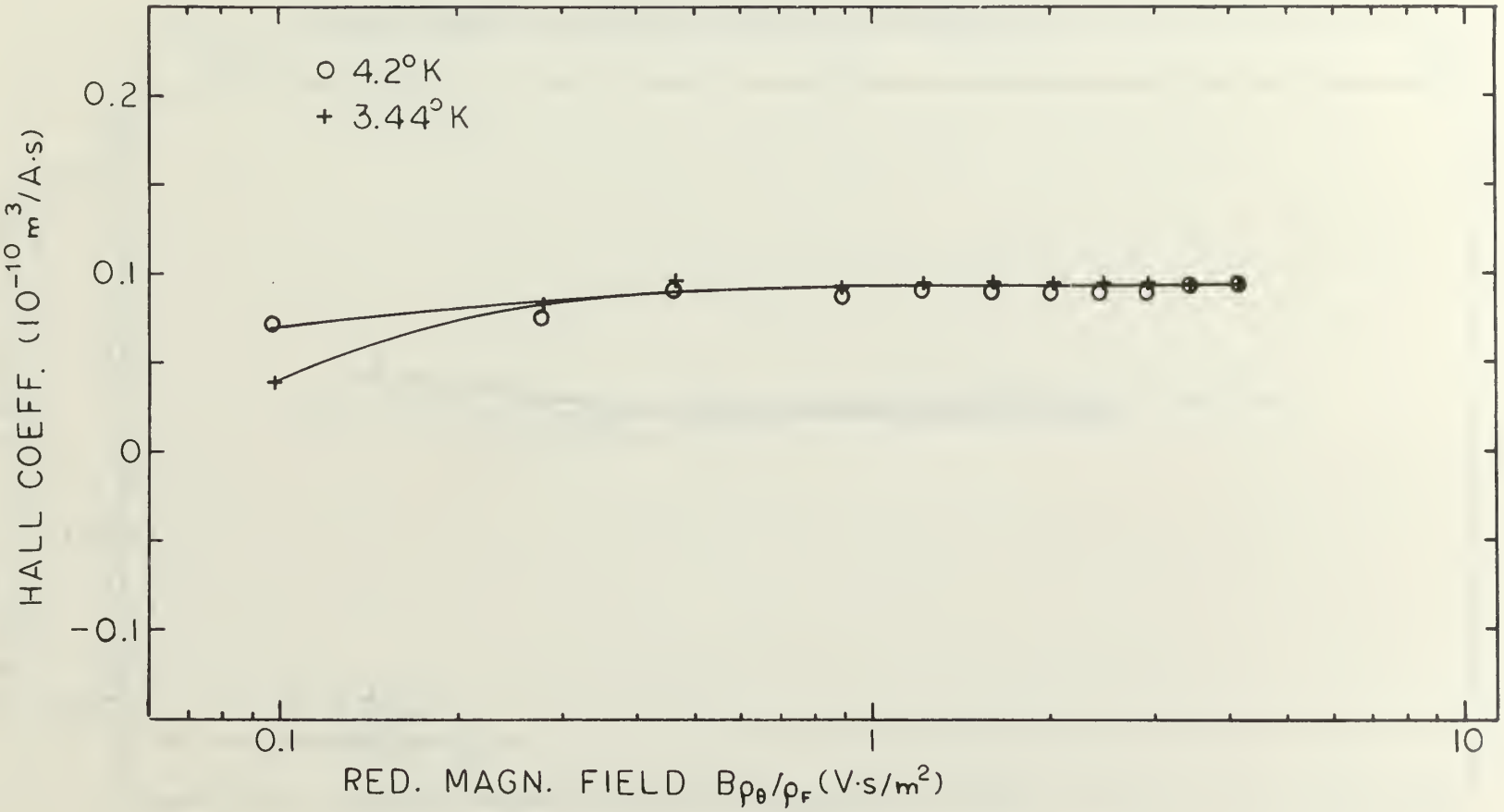

Figure 9. Dependence of Hall coefficient on magnitude of reduced magnetic field for In 3 specimen with I_x = 1000 mamps.

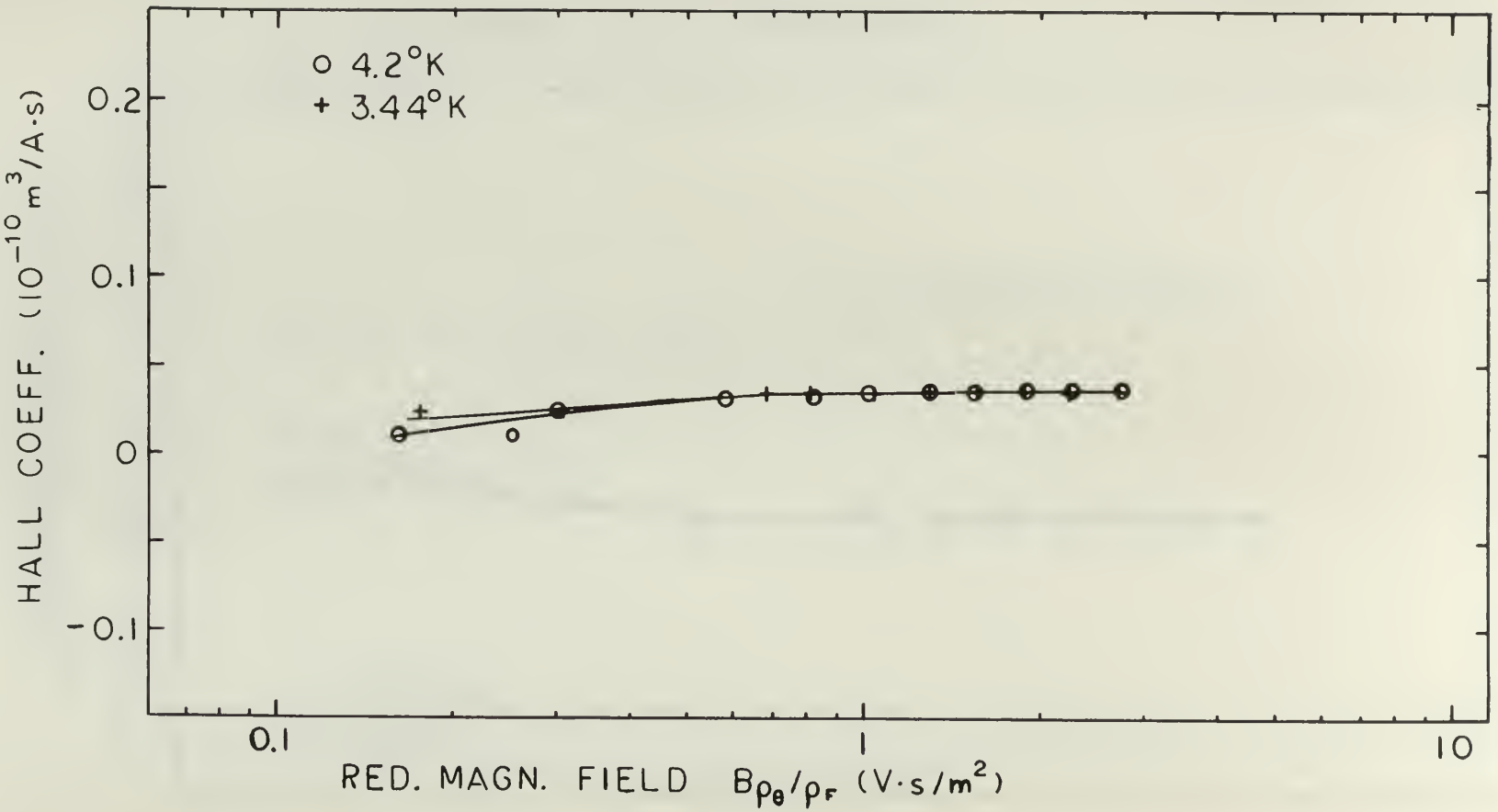

Figure 10. Dependence of Hall coefficient on magnitude of reduced magnetic field for In 4 specimen with I_x = 1000 mamps.

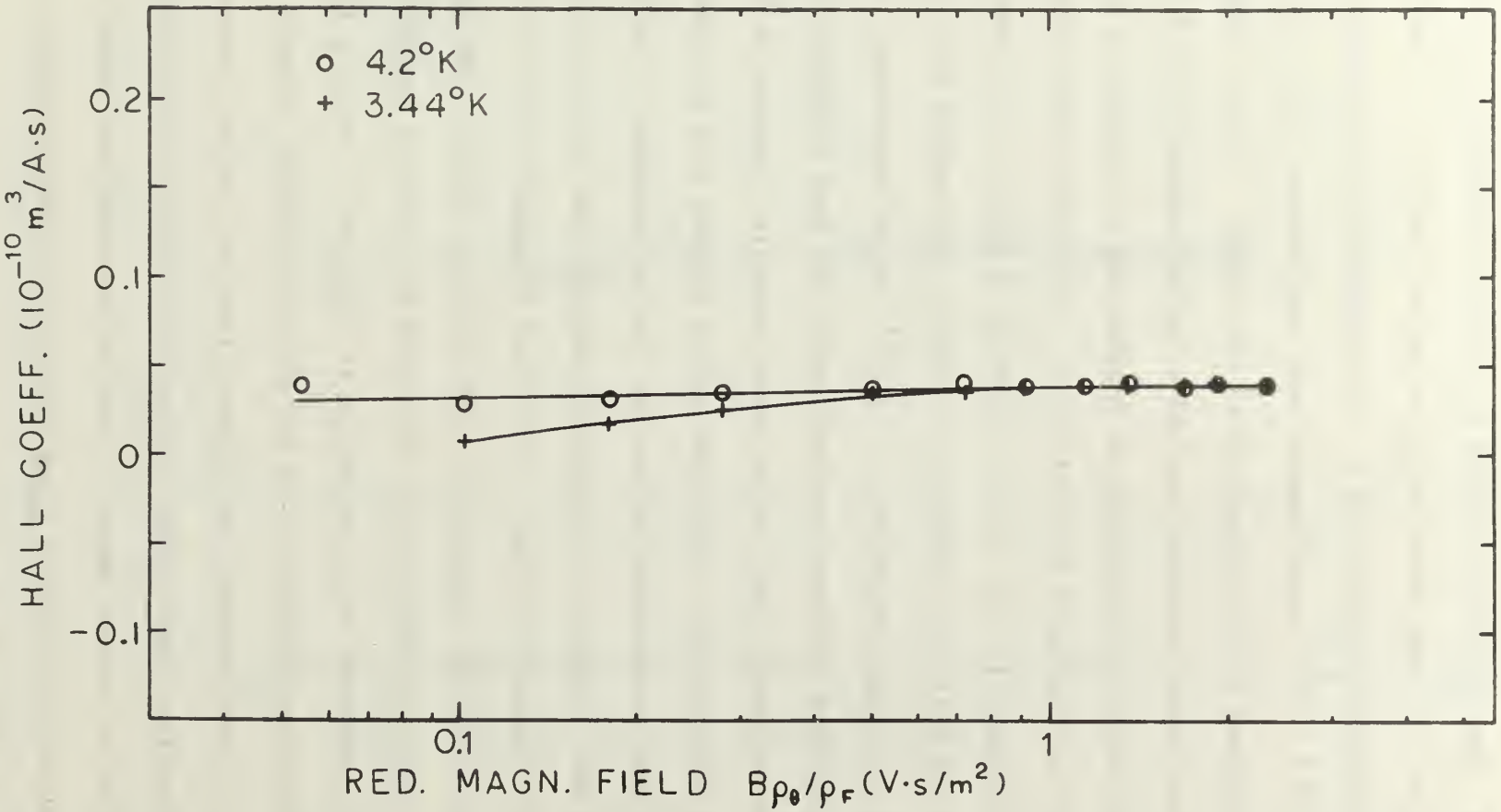

Figure 11. Dependence of Hall coefficient on magnitude of reduced magnetic field for In 6 specimen with I_x = 1000 mamps.

$4.2^{o}K$. The exception occurred on the In-2 specimen (Fig. 5) with $\underline{I}_x$ equal to 250 mamps where the $\underline{R}_H$ values at $3.44^{o}K$ were slightly above the corresponding values at $4.2^{o}K$. The maximum Hall coefficient value ($R_H = 9.1 \times 10^{-12}$ meter^3/ampere-sec) was obtained with In-3, the thickest specimen on which measurements were taken. The Hall coefficient for the thinner specimens reached a smaller maximum (4 to 6 x 10^{-12} meter^3/ampere-sec) although the maximum was not related in a regular manner to decreasing film thickness. No entirely satisfactory curves were obtained for the In-5 ($t = 1900$ Å) specimen, as its null was unstable above the critical temperature. However, the maximum Hall coefficient value for this specimen was 4.3×10^{-12} meter^3/ampere-sec. Since the In-2 and In-4 specimens are very nearly the same thickness, it is of interest to compare data to the extent possible. Looking at Figures 7 and 10 we find the Hall coefficient values for the In-2 specimen slightly above the corresponding values for the In-4 specimen. The Hall coefficient data obtained for evaporated indium films fall just below the results obtained by Cooper, Cotti, and Rasmussen [5] in the low-field region on rolled indium films with thickness greater than 0.08 mm.

Before considering the data below the critical temperature, it is to be noted that this information is displayed in Figures 12-15 for the In-3 specimen, Figures 16-18 for the In-4 specimen, Figures 19 and 20 for the In-5 specimen, and Figures 21-24 for the In-6 specimen. For each specimen these curves display the pseudo Hall coefficient as a function of reduced magnetic field in the weak-field region and the normal Hall coefficient $\underline{R}_H$ as a function of reduced magnetic field in the higher-field region.

In the region below the critical temperature the data measured in

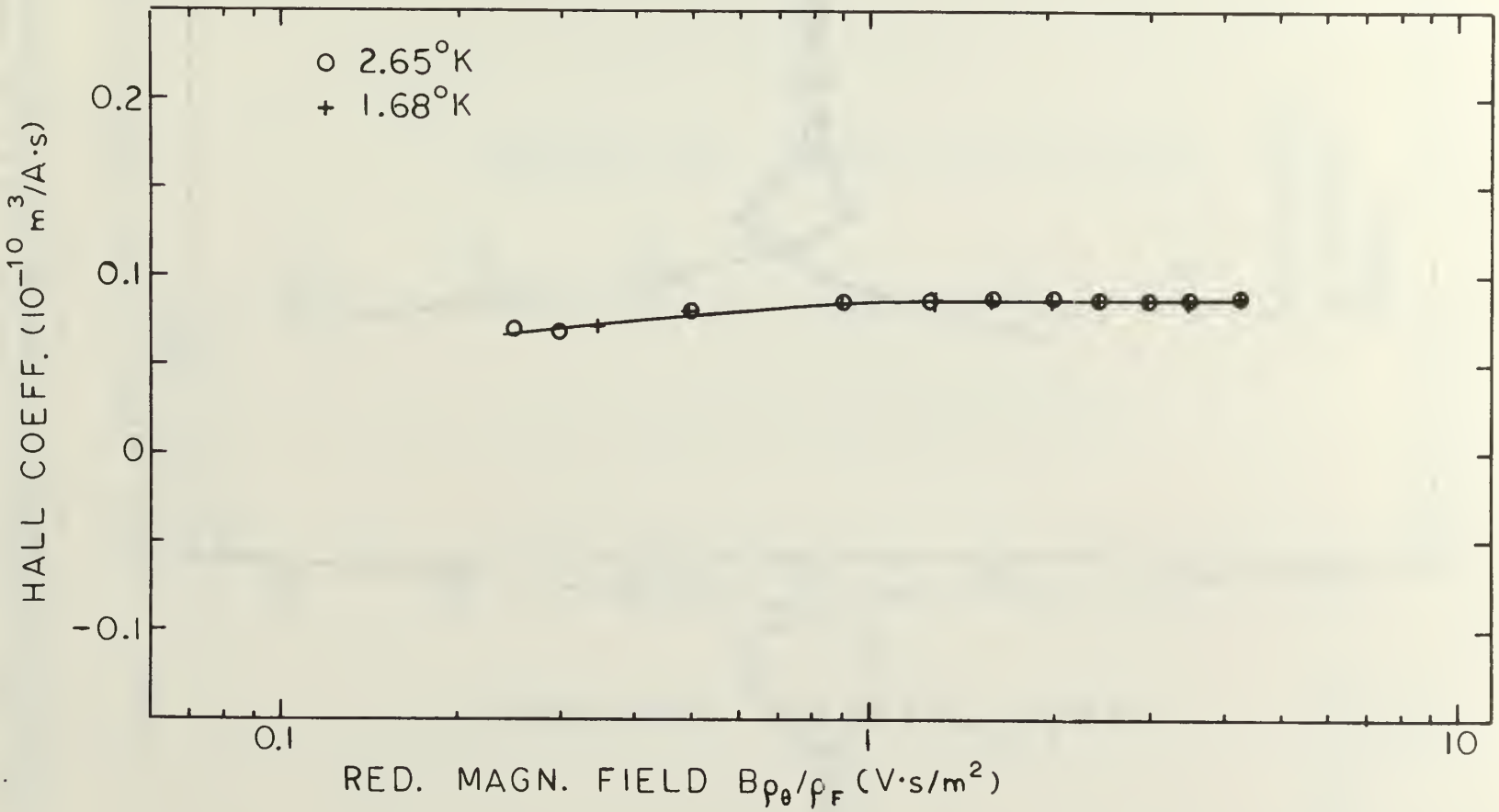

Figure 12. Dependence of Hall coefficient on magnitude of reduced magnetic field for In 3 specimen with I_x = 500 mamps.

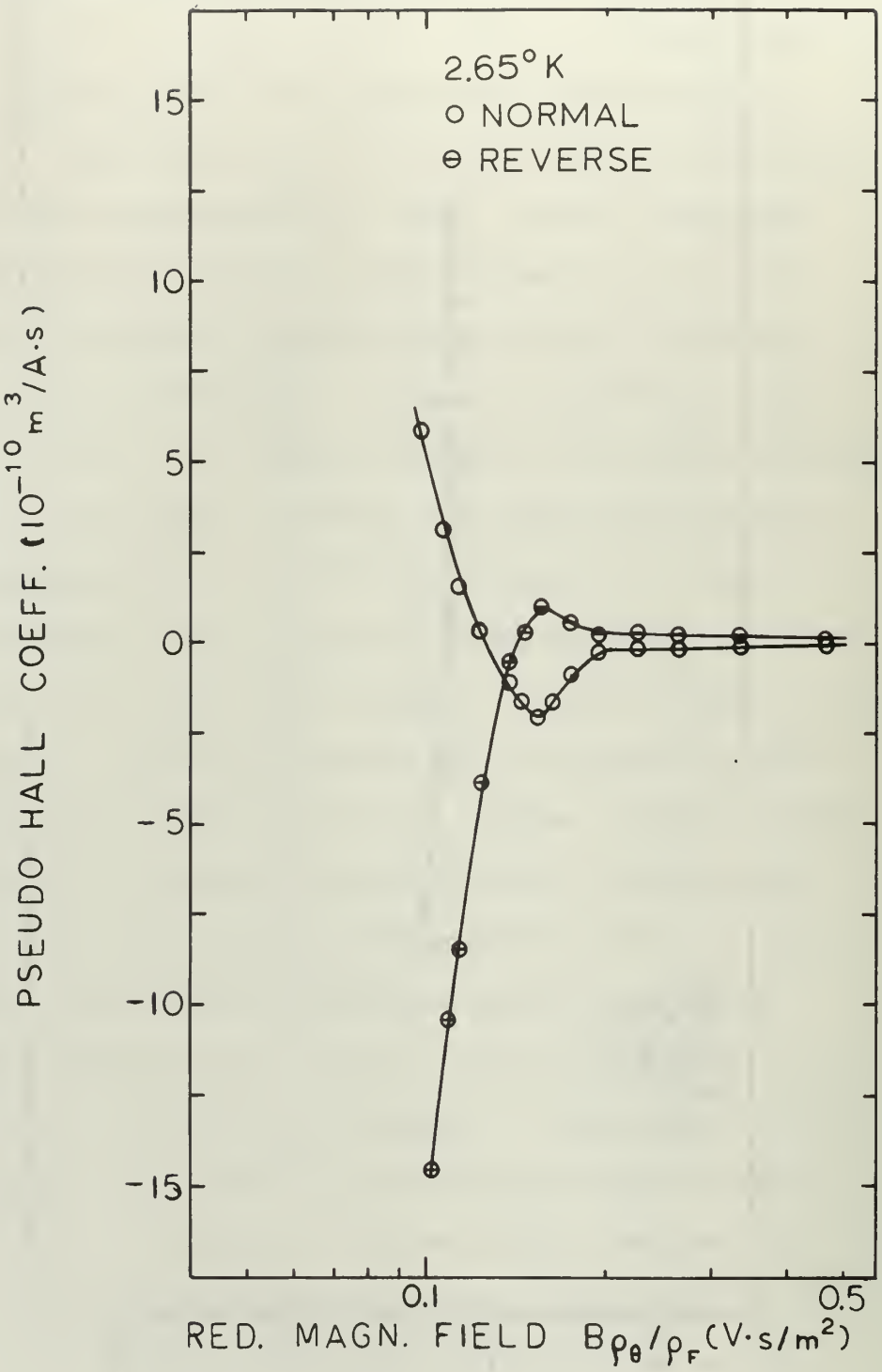

Figure 13. Dependence of pseudo Hall coefficient on magnitude of reduced magnetic field for In 3 specimen with I_x = 500 mamps.

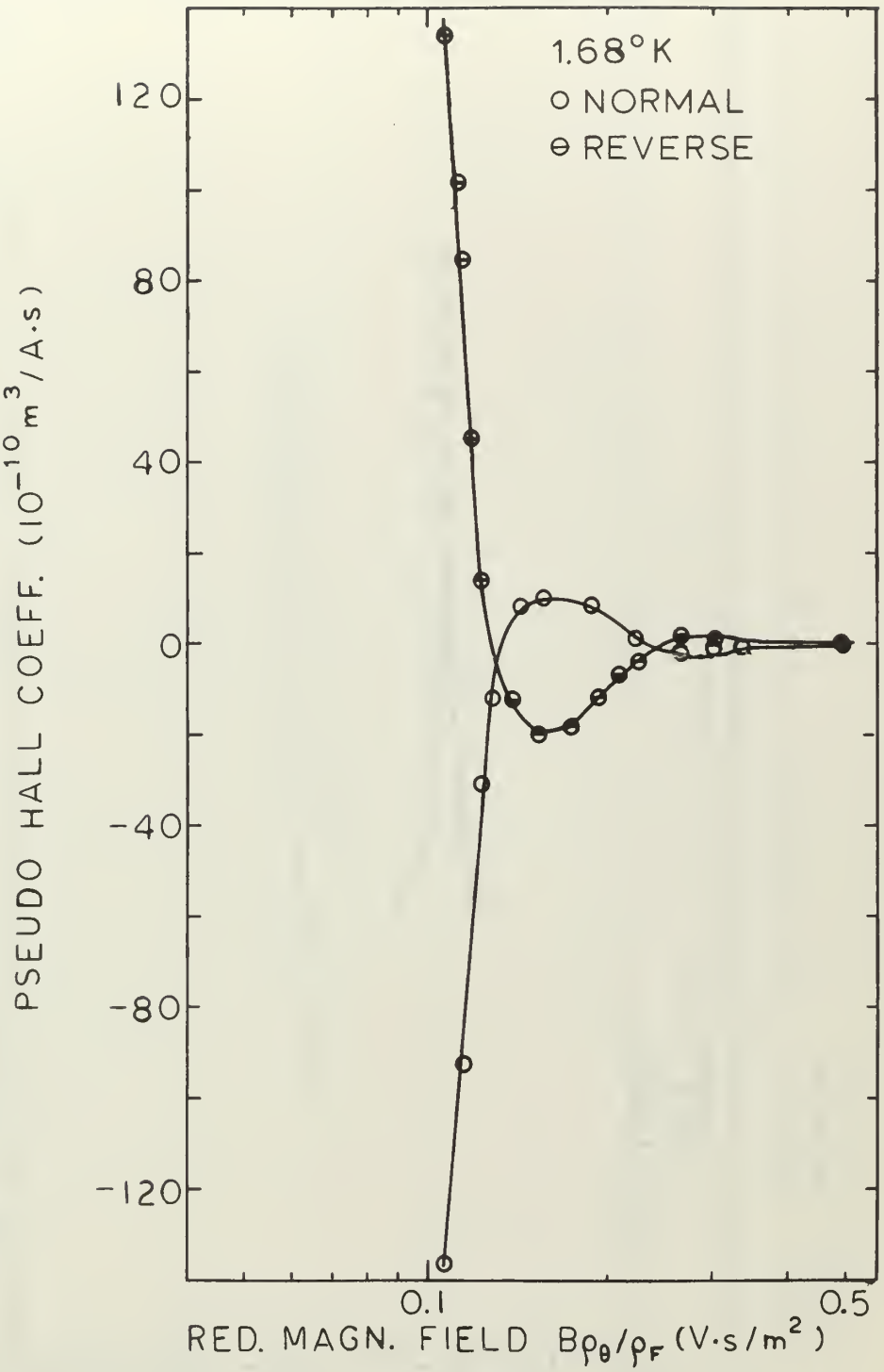

Figure 14. Dependence of pseudo Hall coefficient on magnitude of reduced magnetic field for In 3 specimen with I_x = 500 mamps.

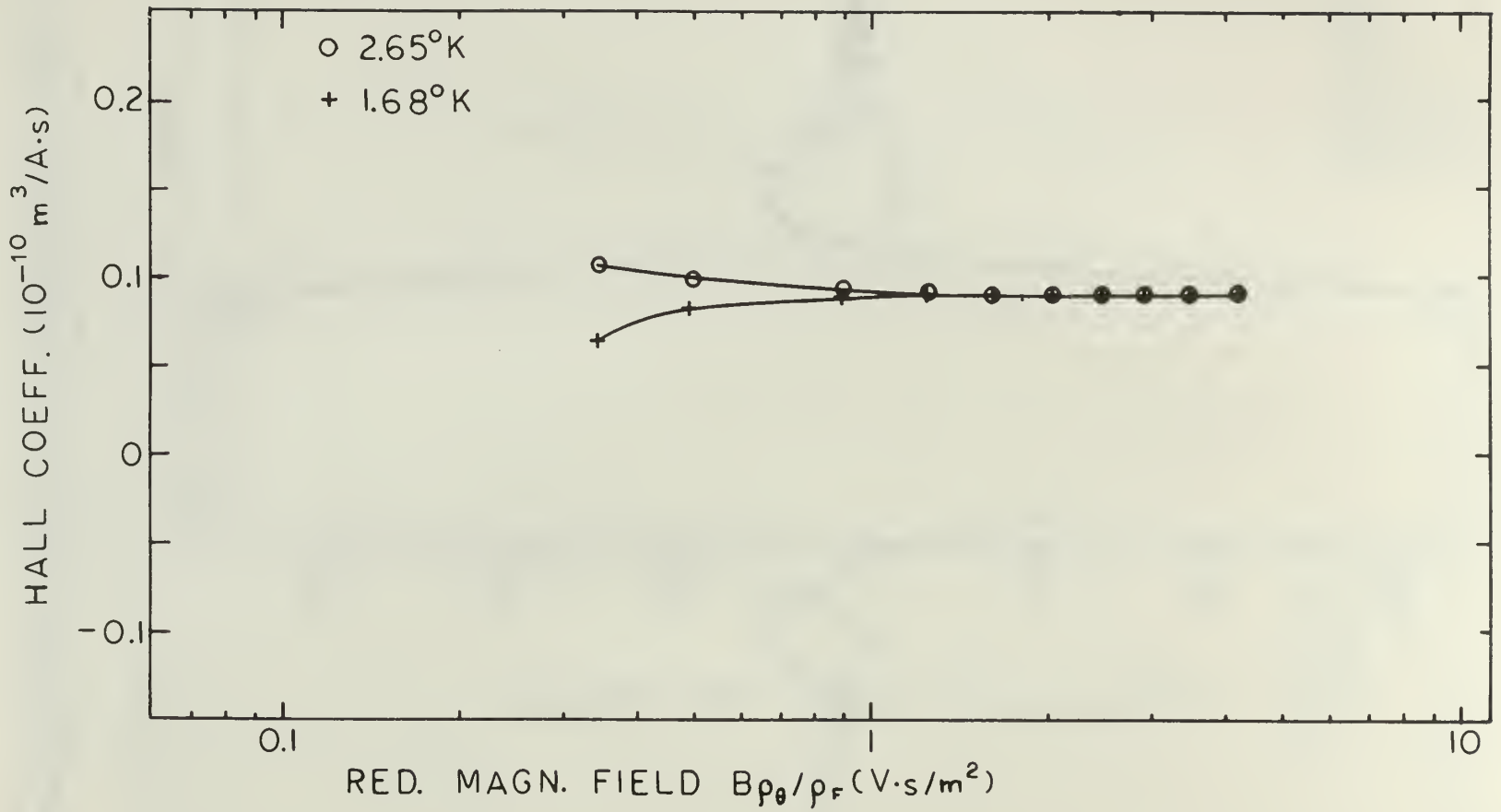

Figure 15. Dependence of Hall coefficient on magnitude of reduced magnetic field for In 3 specimen with I_x = 1000 mamps.

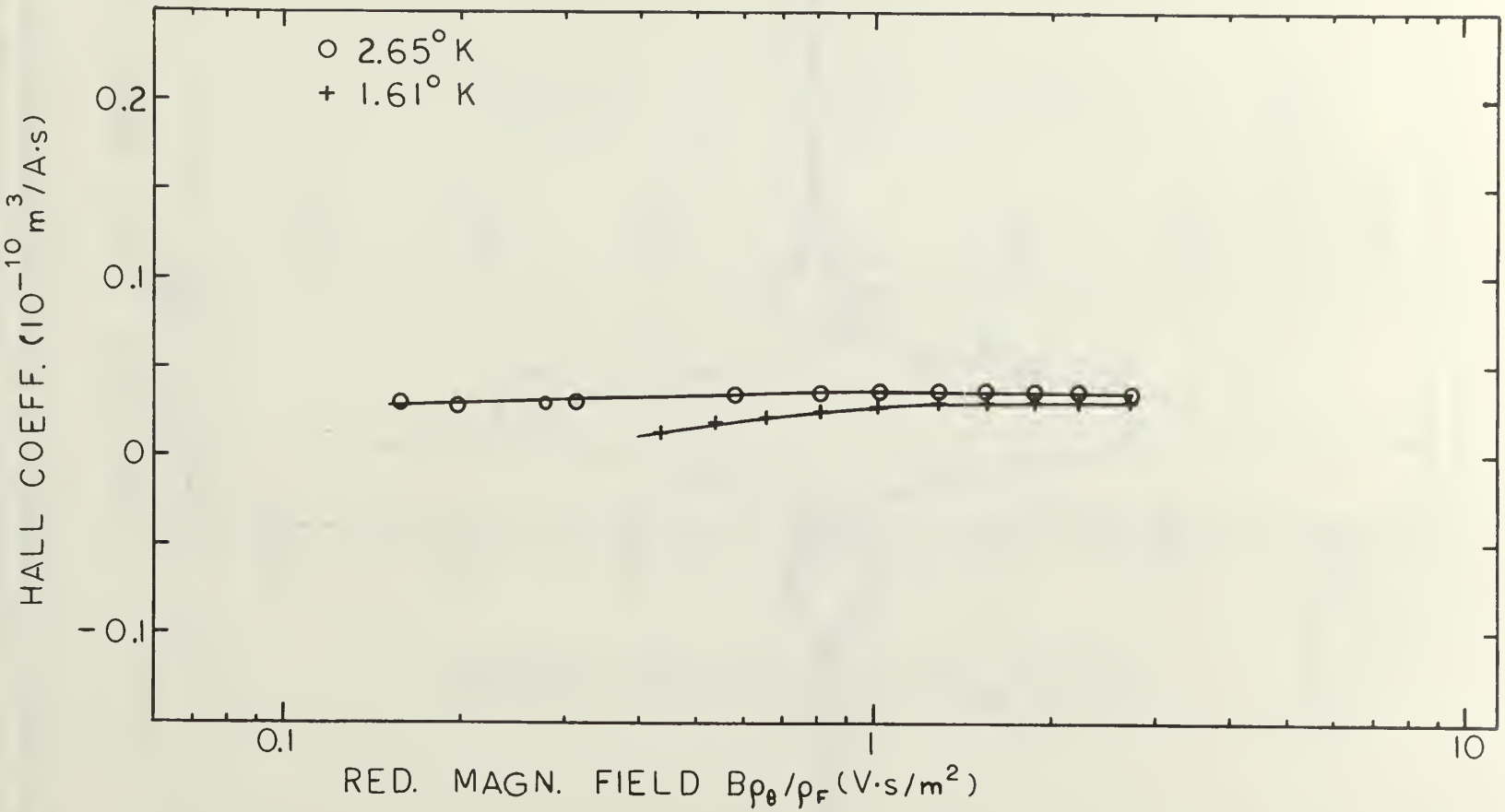

Figure 16. Dependence of Hall coefficient on magnitude of reduced magnetic field for In 4 specimen with I_x = 1000 mamps.

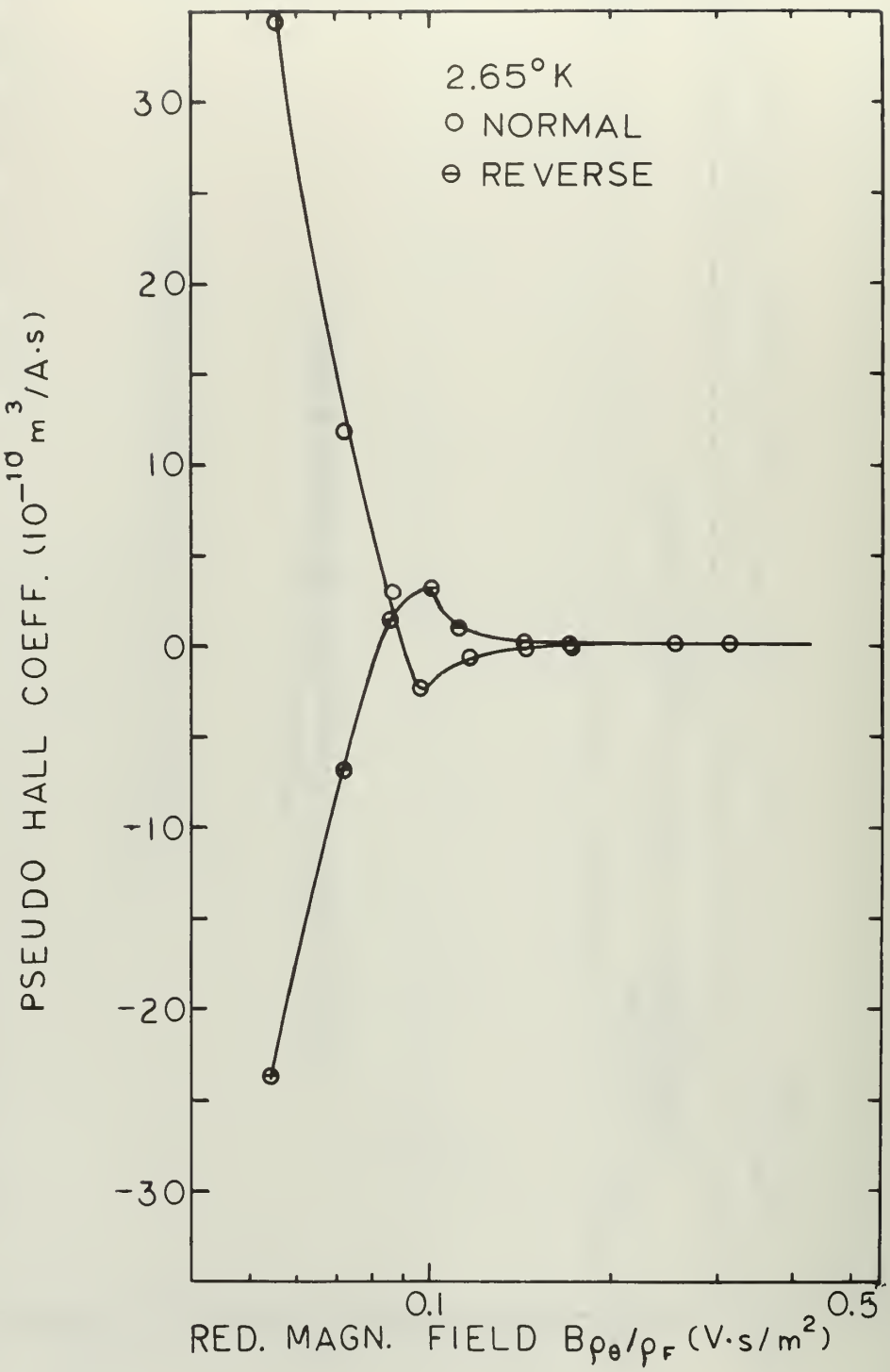

Figure 17. Dependence of pseudo Hall coefficient on magnitude of reduced magnetic field for In 4 specimen with I_x = 1000 mamps.

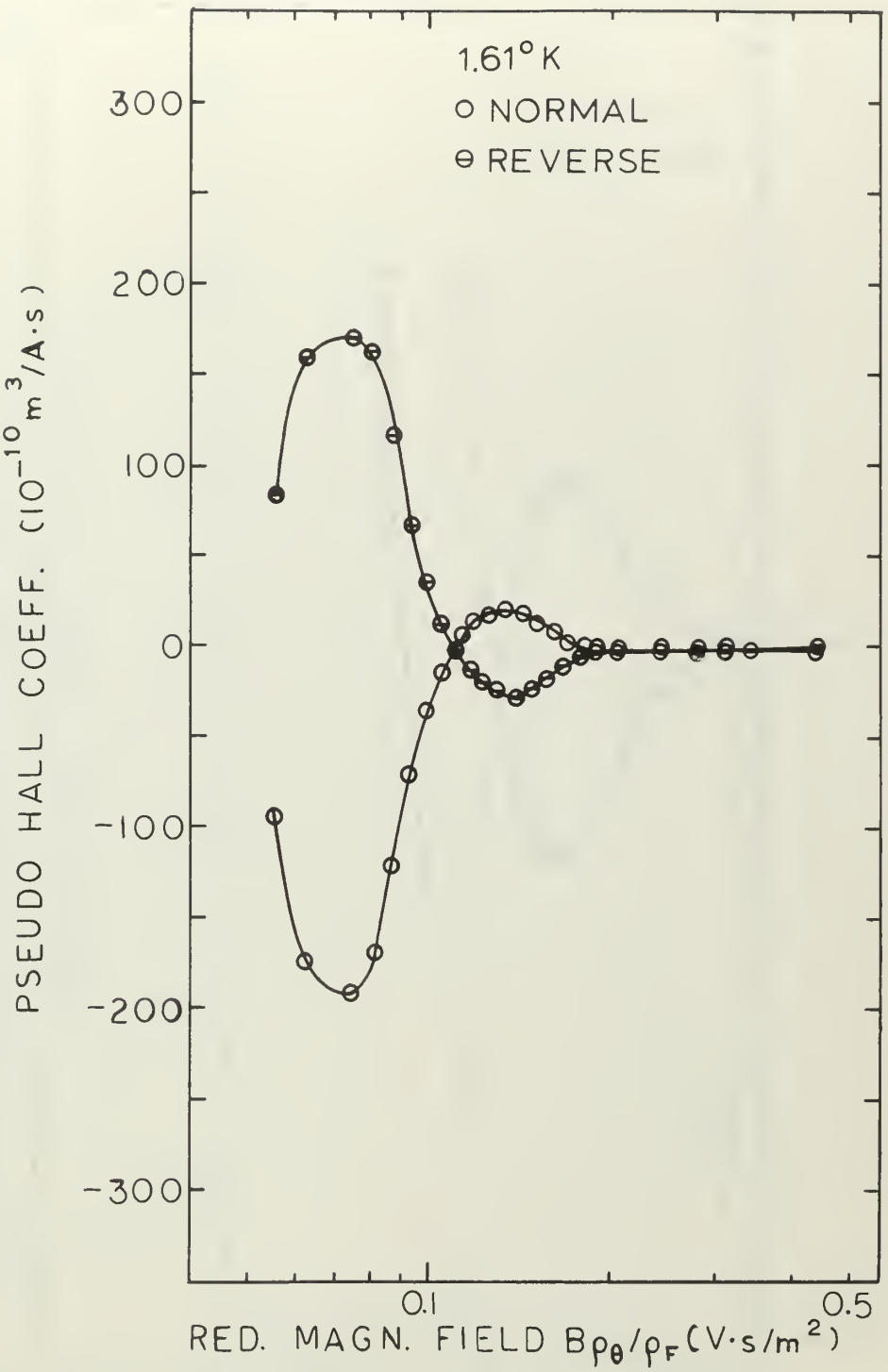

Figure 18. Dependence of pseudo Hall coefficient on magnitude of reduced magnetic field for In 4 specimen with I_x = 1000 mamps.

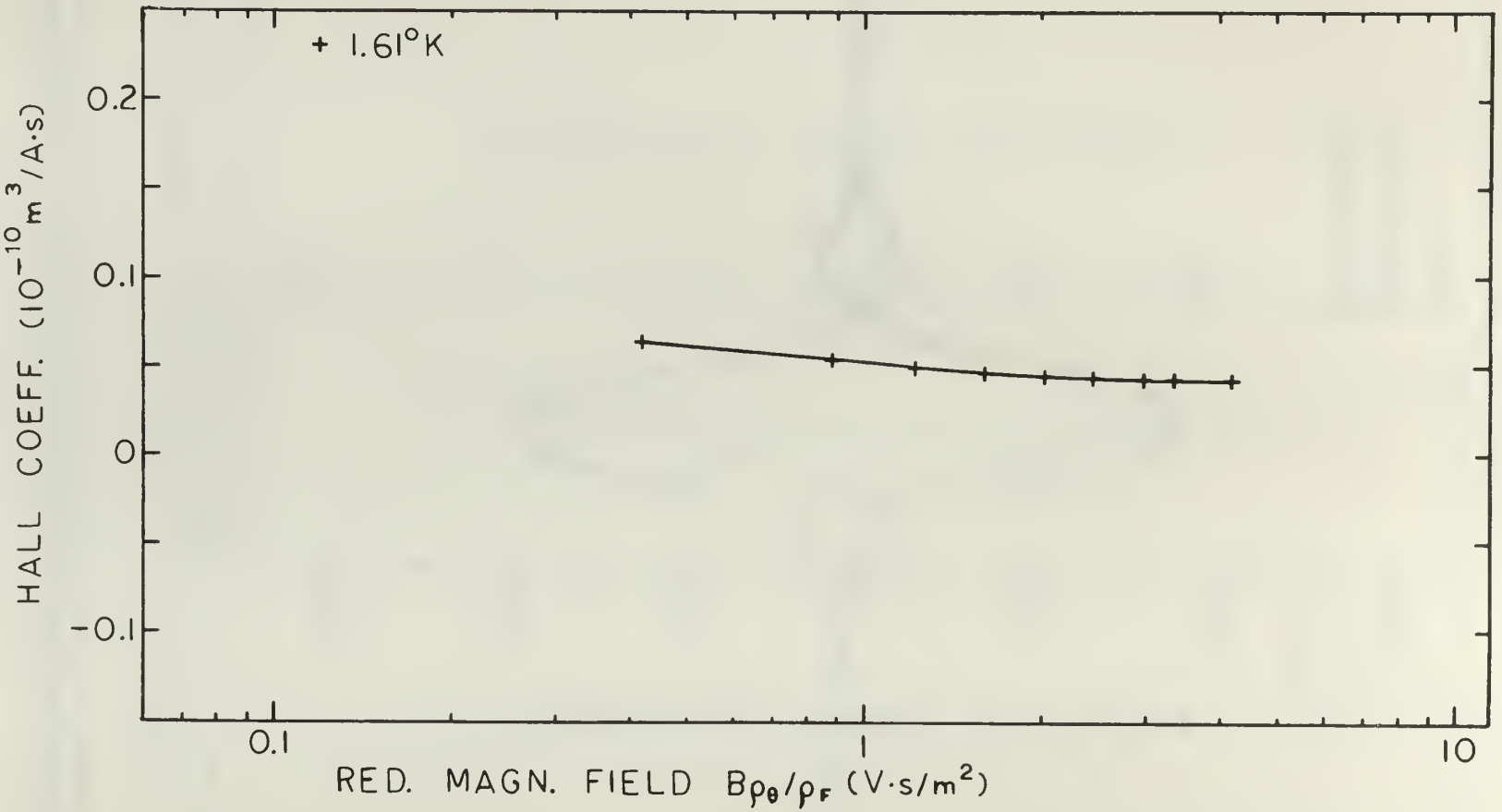

Figure 19. Dependence of Hall coefficient on magnitude of reduced magnetic field for In 5 specimen with I_x = 1000 mamps.

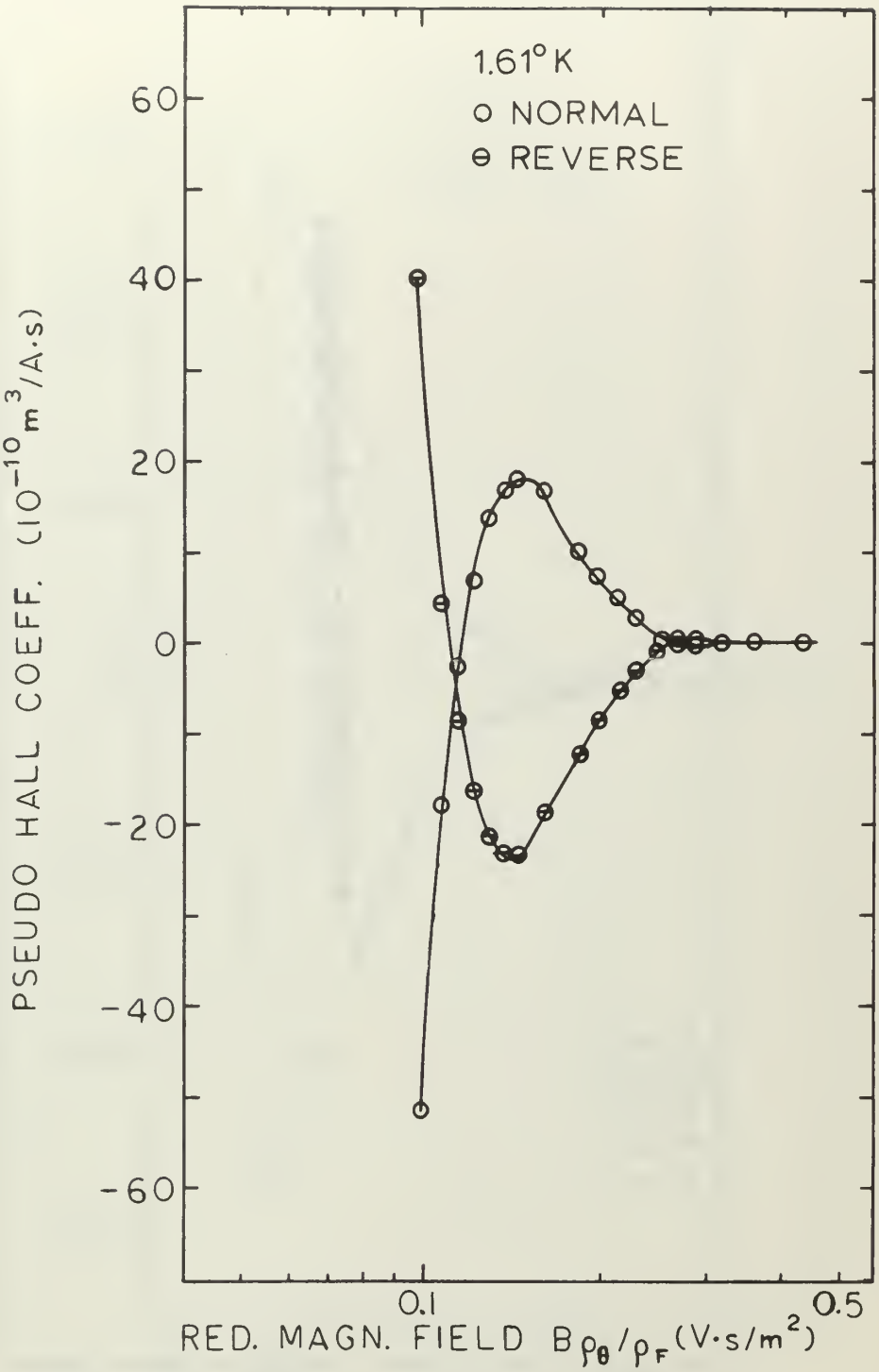

Figure 20. Dependence of pseudo Hall coefficient on magnitude of reduced magnetic field for In 5 specimen with I_x = 1000 mamps.

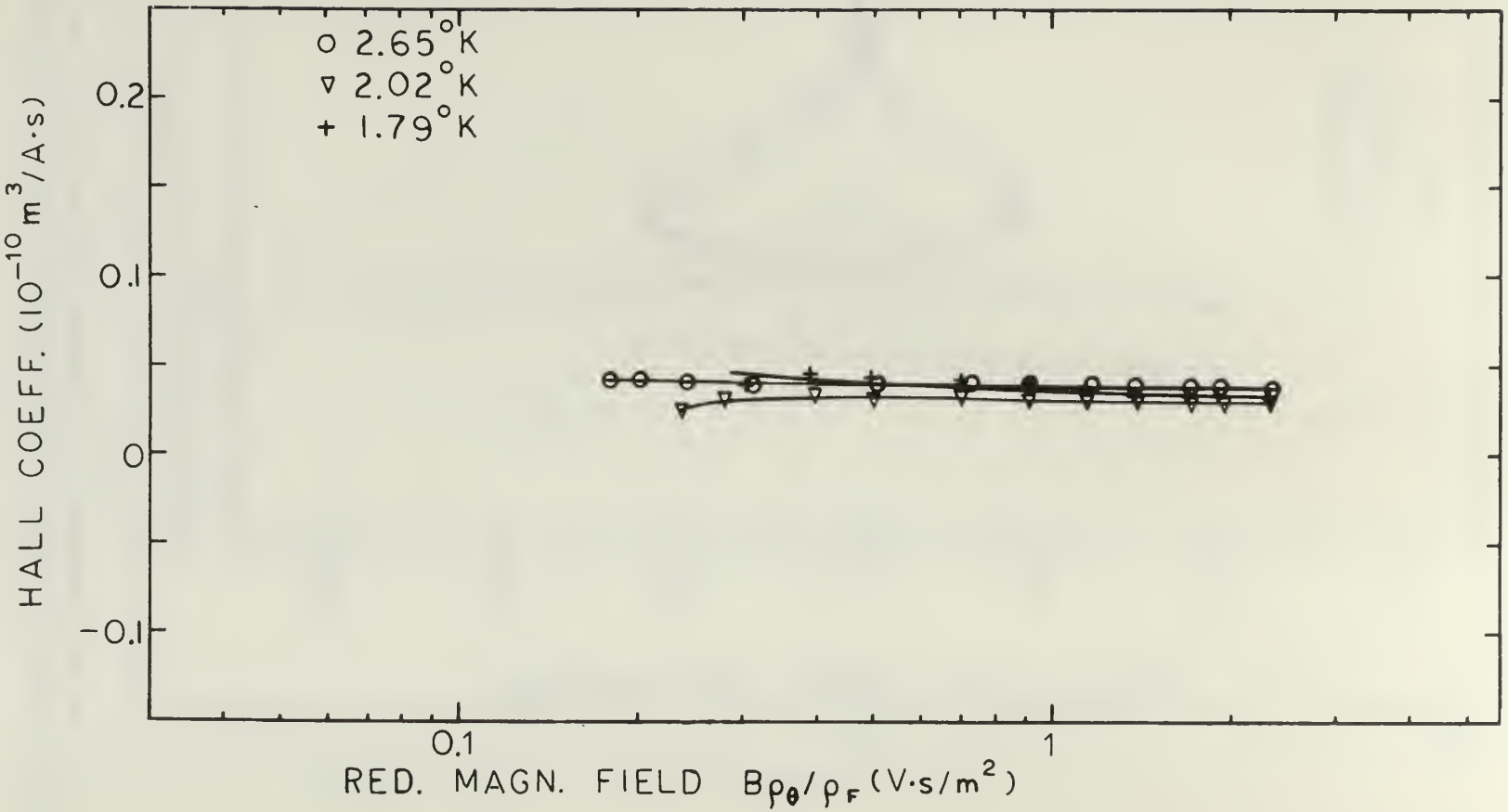

Figure 21. Dependence of Hall coefficient on magnitude of reduced magnetic field for In 6 specimen with I_x = 1000 mamps.

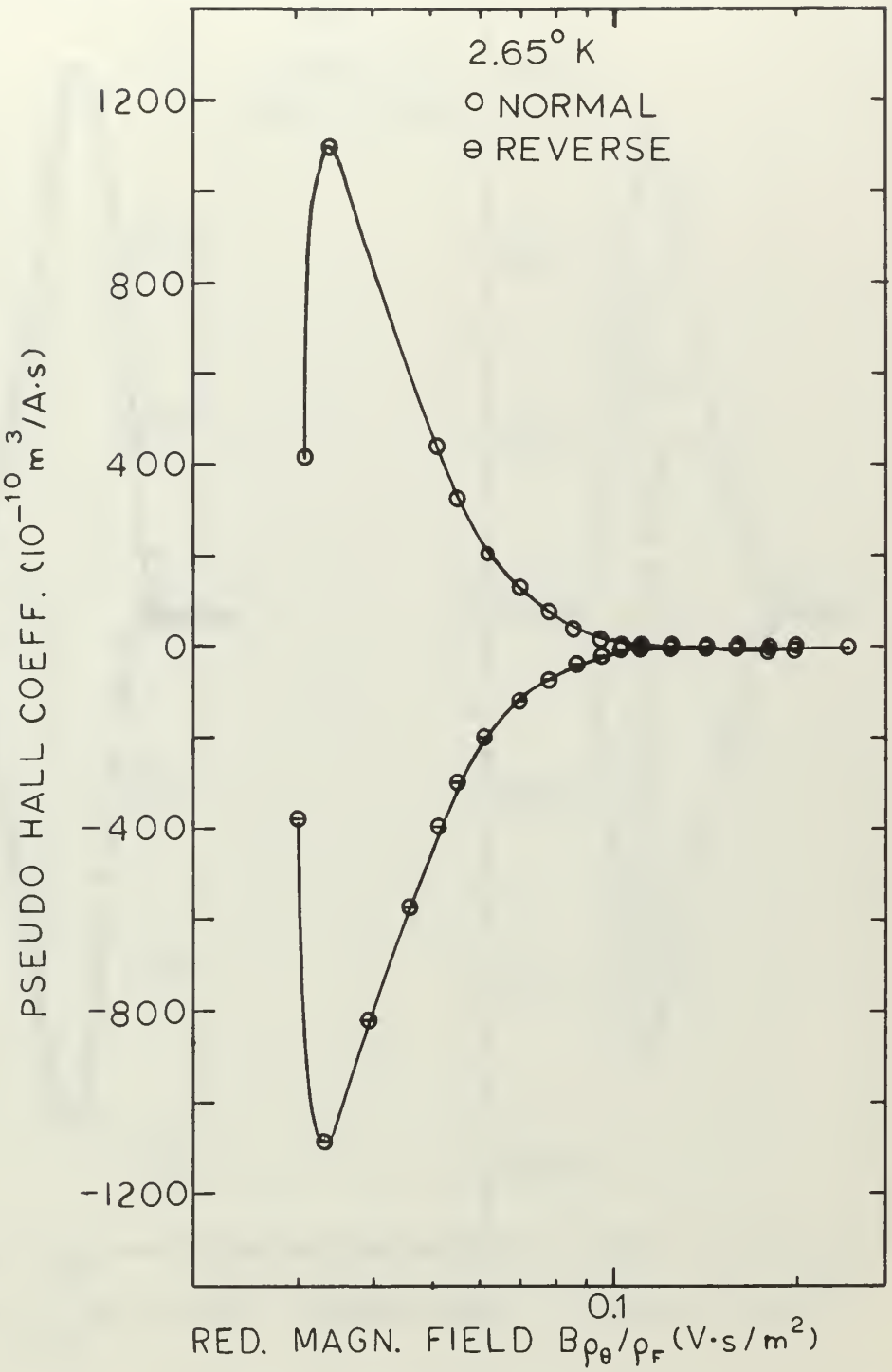

Figure 22. Dependence of pseudo Hall coefficient on magnitude of reduced magnetic field for In 6 specimen with I_x = 1000 mamps.

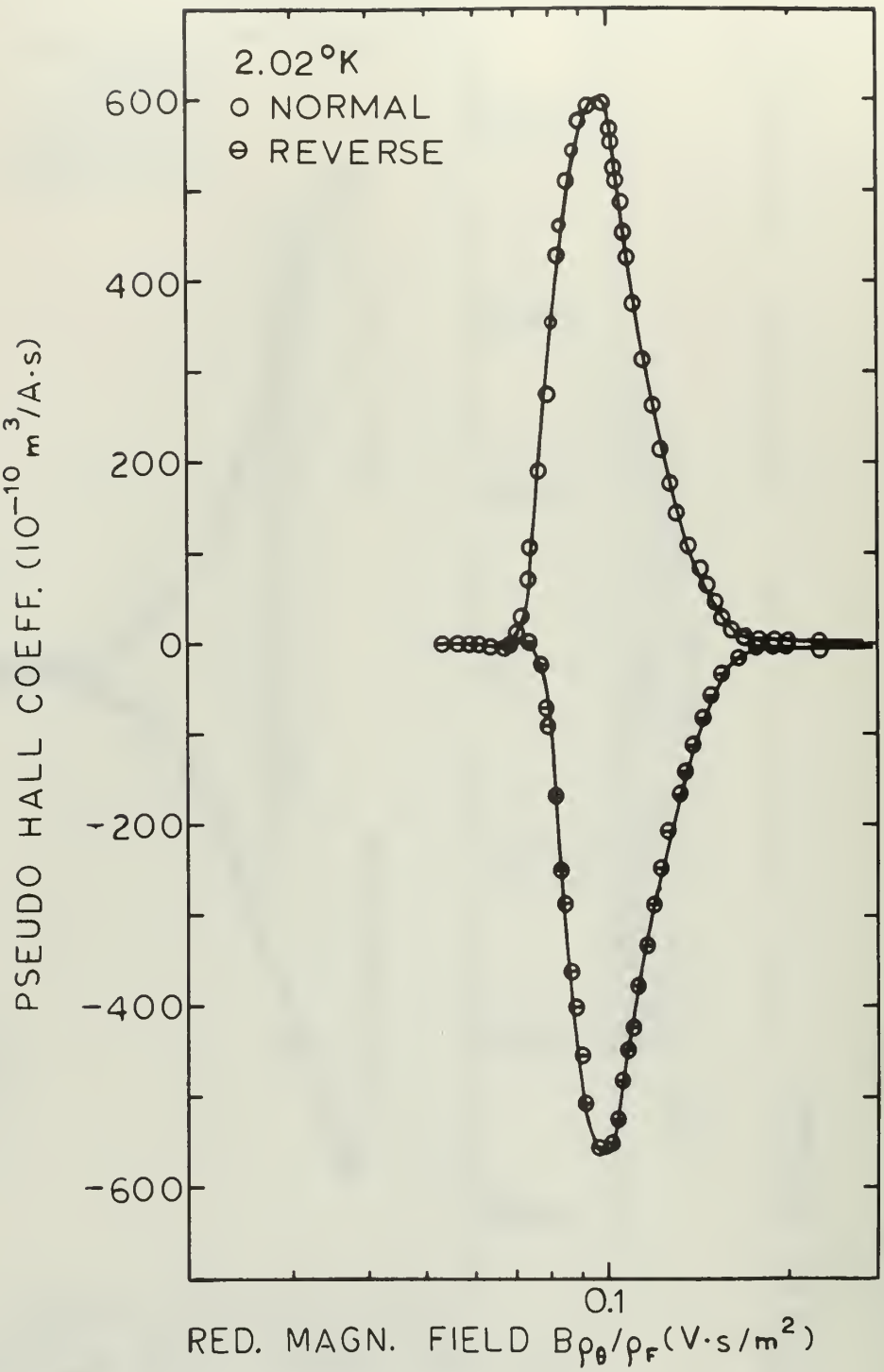

Figure 23. Dependence of pseudo Hall coefficient on magnitude of reduced magnetic field for In 6 specimen with I_x = 1000 mamps.

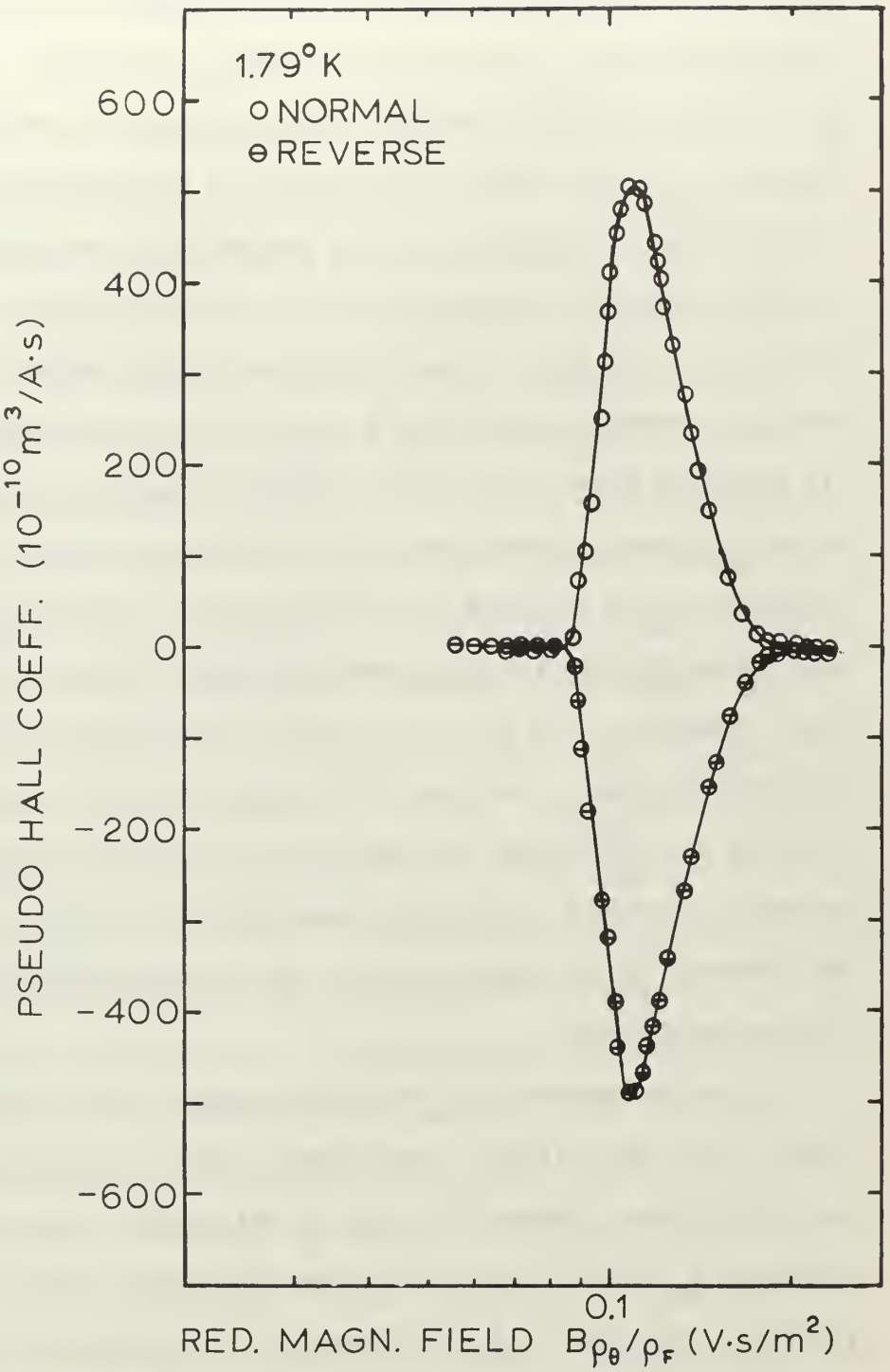

Figure 24. Dependence of pseudo Hall coefficient on magnitude of reduced magnetic field for In 6 specimen with I_x = 1000 mamps.

the higher-field region will be discussed separately and prior to considering the data in the weak-field region. The higher-field region was found to exist when the magnetic field setting was greater than 0.2-0.3 kilogauss. In this region the behavior of the transverse potential $\underline{V}_y$ was reasonable, and the sign of $\underline{V}_y$ changed when the magnetic field direction was reversed. Figures 12, 15, 16, 19 and 21 show a plot of the Hall coefficient $\underline{R}_H$ as a function of the reduced magnetic field for temperatures varying between 2.65°K and 1.61°K. These figures show that all specimens below the critical temperature and in the higher-field region exhibited a normal Hall effect that was positive. The Hall coefficient values obtained in this higher-field region were generally in good agreement with the corresponding results above the critical temperature. However, it is to be noted that on three separate data runs of different specimens, In-3 at 2.65°K (Fig. 15), In-5 at 1.61°K (Fig. 19), and In-6 at 1.79°K (Fig. 21) the Hall coefficient although essentially constant, decreased slowly with magnetic field. This is in contrast to the behavior of all other data runs in this region where $\underline{R}_H$ increased slowly with magnetic field.

If we now consider the weak-field region (less than 0.2-0.3 kilogauss) below the critical temperature, the more interesting and unexpected data were observed to exist in this area. Here the transverse potential $\underline{V}_y$ did not change sign when the magnetic field direction was reversed. The sign of $\underline{V}_y$ did change with a reversal of the specimen current $\underline{I}_x$. In addition to this abnormality, the measured transverse potential $\underline{V}_y$ exhibited the following unusual properties: The magnitude of $\underline{V}_y$ was orders-of-magnitude larger than the Hall voltages measured in the higher-field region, and with increasing field, $\underline{V}_y$ varied in a manner

similar to a damped oscillating function that was aperiodic with magnetic field strength. With the exception of the In-6 specimen the behavior of $\underline{V}_y$ with magnetic field strength was to attain a large peak value in one direction, reverse polarity and pass through one or more smaller peaks in alternate directions and finally approach the normal Hall voltage.

It is of interest to look at the behavior of the specimen resistance with increasing field since the behavior of the transverse potential $\underline{V}_y$ was so very unusual. Figure 25 shows a plot of specimen resistance as a function of magnetic field for the In-4 specimen in the region below the critical temperature. This is a representative plot of the behavior of specimen resistance for all samples. At 2.65°K the specimen resistance was essentially constant throughout the magnetic field range. At the lower temperature, 1.61°K, the specimen resistance at the minimum field was initially only a small fraction of its full value, and it increased in a regular manner with increasing field. When the magnetic field was decreased from maximum to minimum, the resistance curve was not duplicated. At minimum field the resistance was now slightly less than one half of full value. This large difference in resistance as the magnetic field was cycled is due to joule heating in the specimen. The oscillating behavior of $\underline{V}_y$ occurred at 2.65°K where the specimen resistance was constant as well as at 1.61°K where the specimen resistance varied over a wide range. Moreover, except for a small hysteresis, the oscillating behavior of $\underline{V}_y$ was the same for both the increasing and decreasing field directions, even in cases where the specimen resistance was not the same in the increasing and decreasing field directions.

The exception to the behavior of $\underline{V}_y$ which was outlined above, occurred in In-6, the thinnest film specimen tested. Below 2.02°K this

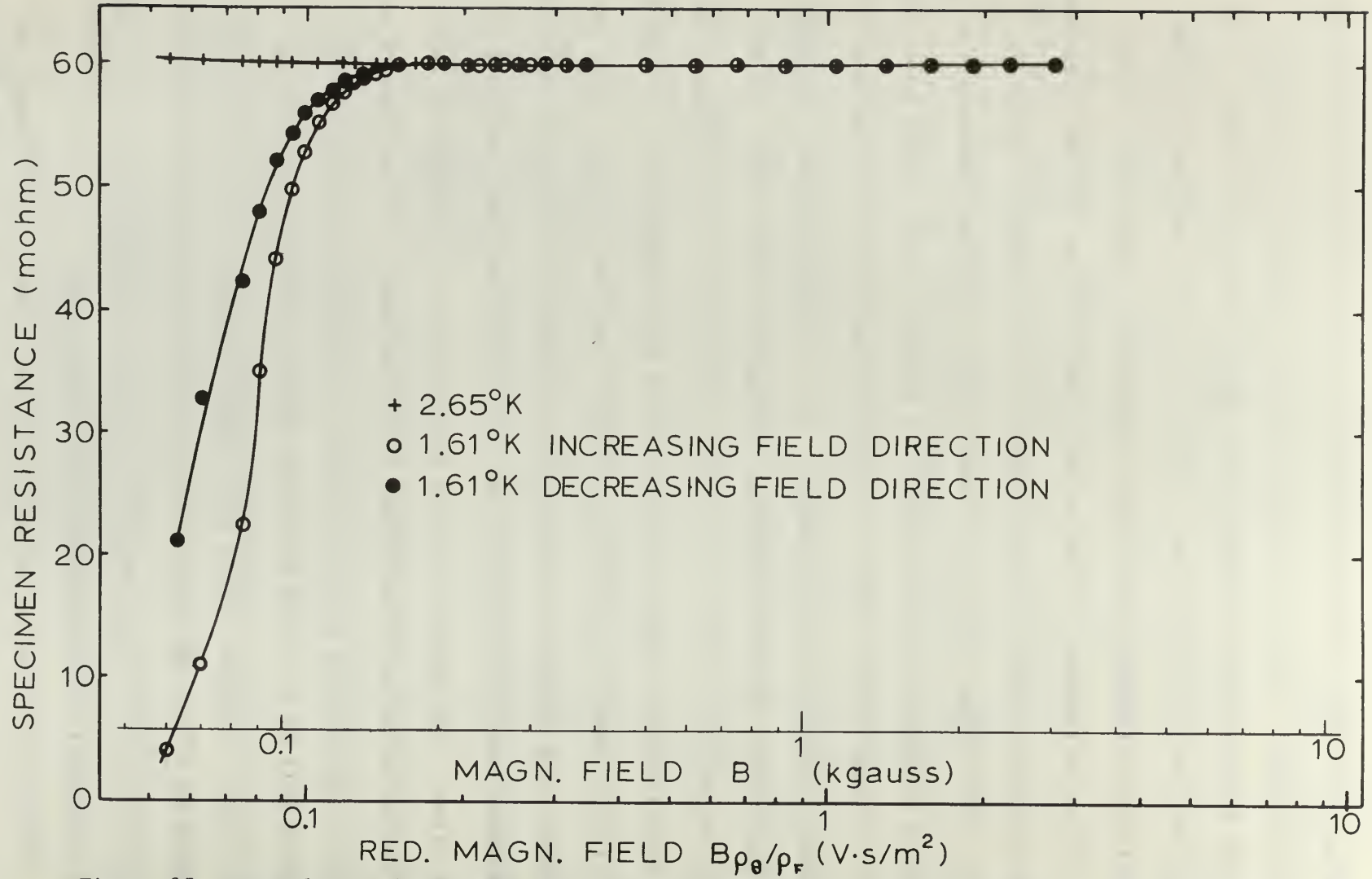

Figure 25. Dependence of specimen resistance on magnitude of reduced magnetic field for In 4 specimen.

specimen was superconductive and exhibited a zero transverse potential $\underline{V}_y$ with minimum magnetic field setting (0.08 kilogauss). The specimen resistance and $\underline{V}_y$ remained zero over a small range of increasing field values (0.08-0.10 kilogauss). As the field continued to increase (0.10-0.12 kilogauss), $\underline{V}_y$ remained at zero even though the specimen resistance increased to a small but finite value. With a further increase in magnetic field non-zero $\underline{V}_y$ readings were obtained, and the specimen resistance continued to rise and become fully developed at 0.3 kilogauss. For this specimen $\underline{V}_y$ initially reached a very small peak value in one direction. It then reversed polarity and attained a very large peak value in the opposite direction. $\underline{V}_y$ then decreased directly to the value of the normal Hall voltage without reversing polarity for the normal magnetic field direction, but when the magnetic field direction was reversed $\underline{V}_y$ reversed polarity as it decreased. (See Figure 3 for definition of normal and reverse magnetic field directions.)

The strange and unexpected behavior of the transverse potential $\underline{V}_y$ in the weak-field region has been reflected in the data which are displayed in Figures 13, 14, 17, 18, 20, and 22-24. These curves show a plot of pseudo Hall coefficient $\underline{V}_y t/\underline{I}_x \underline{B}_z$ as a function of reduced magnetic field strength $\underline{B}\rho_\Theta/\rho_F$. In normalizing the magnetic field, the fully developed specimen resistance was utilized throughout, even though at the lowest temperature runs the specimen resistance varied over a wide range. These figures display the pseudo Hall coefficient for the magnetic field in the normal direction and also for the field in the reverse direction. It is readily seen that reversal of the magnetic field produces a good mirror image of the pseudo Hall coefficient. Figures 13, 14, 17, 18, and 20 show the pseudo Hall coefficient oscillating in

sign, the peaks becoming smaller and then damping out with increasing field. Figures 22, 23, and 24 for the In-6 specimen show the pseudo Hall coefficient having only one large peak before decreasing to the normal Hall coefficient. The latter two figures show the zero value and the barely discernible initial peak for the pseudo Hall coefficient that was observed on the In-6 specimen below 2.02°K.

Some general observations are applicable in the weak-field region below the critical temperature. The normal Hall effect, if present at all in this region, was completely obscured by the large voltages that were independent of magnetic field direction. It appears that the behavior of the pseudo Hall coefficient is independent of the variation of specimen resistance, since the same behavior of the pseudo Hall coefficient was observed at 2.65°K where the specimen resistance was fully developed and at 1.6°K where it was not. Moreover, as the temperature was decreased, the pseudo Hall coefficient damped out at higher-field values for all specimens. That is, the oscillating behavior of $\underline{V}_y$ in the weak-field region extended to higher-field values as the temperature decreased. This is clearly shown for In-6 on Figures 22, 23, and 24 where the large peak shifts to the right with decreasing temperature. The pseudo Hall coefficient is orders-of-magnitude larger than the normal Hall coefficient measured in the higher-field region. In comparison to the normal Hall coefficient, the peak value of the pseudo Hall coefficient for the In-3 specimen was greater by a factor of 100 at 2.65°K and a factor of 1200 at 1.68°K. Similarly the peak pseudo Hall coefficient value for the In-4 specimen was greater than $\underline{R}_H$ by factor of 250 and 2000 for the corresponding temperatures. Also, with the exception of the In-6 specimen, the minimum magnetic field (0.08 kilogauss)

was too large to permit the samples to remain superconducting below the critical temperature.

A final interesting occurrence in the behavior of the pseudo Hall coefficient was observed on the In-3, In-4, and In-5 specimens. As shown on Figures 13 and 14 for the In-3 specimen and Figures 17 and 18 for the In-4 specimen, the polarity of the pseudo Hall coefficient in the weak-field region changed sign as the temperature was decreased from $2.65^{\circ}K$ to $1.6^{\circ}K$. For the In-5 specimen there was a change in sign in pseudo Hall coefficient as the temperature decreased from $2.65^{\circ}K$ to $2.31^{\circ}K$, and another reversal occurred as the temperature was lowered to $2.09^{\circ}K$. However, a check for this phenomenon was made for the In-6 specimen, and no reversal in polarity of the pseudo Hall coefficient was observed as the temperature was varied below the critical temperature.

5. Conclusions.

Above the critical temperature the Hall coefficient for evaporated indium films was positive for all sample specimens, and its value was essentially constant with increasing magnetic field. The Hall coefficient data for evaporated films were somewhat below the results published by Cooper, Cotti, and Rasmussen [5] for reasonably thick films in the low-field region. With the evaporated films, no crossover to negative values of Hall coefficient were observed. Differences between the current experimental data and the rolled film results were expected, since for evaporated films the ratio of dc resistivity at room temperature (ρ_{293}) to resistivity at 4.2°K (ρ_F) varied between 20 and 40 in comparison to ratios between 2×10^3 and 13×10^3 for rolled films. The experimental data did not correspond to Sondheimer's [7] theoretical calculations for a one-carrier situation, which shows the Hall coefficient in the low-field limit increasing with decreasing film thickness. The actual Hall coefficient in the low-field limit decreased slightly with decreasing thickness for the evaporated films discussed here.

Below the critical temperature there are no known published data on the behavior of the Hall coefficient in indium, and theoretical investigations in this region are lacking owing to the complexity of the problem. Above a reduced magnetic field level of 0.2-0.3 volt-second/meter^2 a normal Hall coefficient was observed, and the data were in good agreement with the corresponding measurements above the critical temperature. Below this magnetic field level, a pseudo Hall voltage was observed, which was independent of the magnetic field direction but was effected by the direction of current flow. The phenomenon observed in this region was of great interest, in part because it was completely

unexpected. However, the physical mechanism which is responsible for the pseudo Hall coefficient is not understood at this time.

Appendix I

Specimen Preparation.

The specimens utilized in this experiment were all laboratory-produced by the authors using standard vacuum evaporation techniques as detailed in both Holland [11] and Summer [12]. The vacuum system employed was that described by MacDowell and Martin [13] as modified by Bower and Simila [14]. The substrates were plexiglas acrylic plastic cut from an 1/8 inch thick sheet to dimensions of 12 cm by 3.4 cm. The connections, made as described in Appendix II, provided an active film length between the power leads of 10 cm, with a distance of 8.5 cm between the connections used for resistance determination. A razor blade mask (Appendix II), employed to give the longitudinal edges of the film the desired configuration, limited the film width to 2.4 cm. Initially, substrates were cleaned with benzol and acetone. However, as it was noted that acetone had a tendency to etch the plexiglas, cleaning was subsequently done with alcohol and benzol, de-ionized water being used as the final cleansing agent.

The indium source material used was a spool of 99.999% pure indium wire with a diameter of 0.050 inches. After cleaning with acetone, a length of wire estimated to have the correct mass was cut from the spool. Accurate determination of the mass was made using an analytical balance (Sartorius Single Pan Analytical Balance, Model 2603, Brinkmann Instruments, Westbury, N. Y.). The wire was then balled up and placed in the evaporation chamber in a slightly dimpled molybdenum boat (Plansee Metalworks, Joint Stock Company, Reutte, Tirol, design number 62.9374).

To minimize film contamination, the ball of indium wire was melted under vacuum and prior to evaporation of each sample with a protective

flag in place covering the substrate. Additionally, the lower trap on the evaporation chamber (diffusion pump suction trap) was filled with liquid nitrogen, but the wells in the top plate of the vacuum jar were not filled. After the wire ball was melted and the pressure in the chamber had decreased to the pre-melting value or less, the wells in the top plate were filled with liquid nitrogen.

For all specimens, evaporation rate and heating current employed were similar, pressure in the chamber being maintained on the 10^{-7} torr scale.

Calculation of the film thickness was done by considering the substrate as a plane surface and the ball of indium wire in the boat after melting as a small directed surface source. From the development given in Holland [11], the thickness of the film above the source t_o is given by

$$t_o = \frac{m}{\pi \rho} \cdot \frac{1}{h^2} \tag{15}$$

where m is the mass evaporated, ρ its density, and h the perpendicular distance from substrate to source. For all samples produced, ρ was 7.28 grams/cm^3 and h was 26.4 cm. The value obtained for t_o was used as the film thickness t in all calculations. Inasmuch as the same geometry was used in production of all specimens, relative thicknesses are more certain than absolute thicknesses.

Appendix II

Specimens.

All specimens used in this investigation were manufactured by the authors utilizing the vacuum evaporation technique (detailed in Appendix I). Film thickness was computed for each specimen from the method described therein. This Appendix covers the choice of substrate material and the methods employed in making the satisfactory, reliable electrical connections to the film that were needed for instrumentation and power leads. Obtaining and maintaining this electrical contact was the major obstacle encountered in the conduct of this investigation.

In order to determine which was the more suitable substrate material from the viewpoints of resultant film and ease of attaching and maintaining the electrical connections, initial sample specimens were made using both glass microscope slides and plexiglas acrylic plastic. These two materials were selected owing to their availability, and their coefficients of expansion which were comparable to that of indium; the latter factor being of importance owing to the wide range of temperatures that would be experienced by the specimen ($1.5^{o}K$ to $300^{o}K$). Poorly matched coefficients between substrate and film could easily cause cracking or buckling of the film with resultant large non-uniformities or loss of continuity. Testing of both sample specimens in liquid nitrogen indicated that, with respect to operating temperatures, either glass or plexiglas would be an acceptable material for a substrate.

Although the film on the glass substrate appeared visually to be somewhat more uniform than the one on plexiglas, the difficulty of making electrical connections to the glass substrate resulted in the selection of plexiglas as the substrate material.

The initial means of making contact with the film on the plexiglas substrate consisted of imbedding the connections for the power leads in two grooves or slots (one at each end of the sample) cut across the face of the substrate perpendicular to the desired current flow path. Leads were brought in from the side of the substrate through an "L" shaped tunnel that connected the side of the substrate with the film area. The copper power leads were "tinned" with indium, and then covered over in the slots with a melt of indium from the same spool of wire as that used for the film. The copper instrumentation leads were also "tinned" with indium, inserted into the side holes, and then these side holes as well as the connecting top holes were filled with an indium melt as had been done with the power leads. The indium was thus bonded to the leads through this melting process. Excess indium was removed from over the slots and holes to restore a flat surface to the plexiglas before depositing the film on it. Thus the indium sample material could be deposited on a plane surface, making contact with indium filler material, which surrounded the power and instrumentation leads simultaneously with formation of the film on the substrate.

These contacts proved to be unreliable, and had little inherent strength. Despite careful handling in removing the specimen from its mounting in the evaporation chamber and connecting it to the test assembly, continuity was often lost. It could be restored, in some instances, by melting a small amount of indium over the contact with a low-temperature soldering iron. This method did not always prove satisfactory, as damage easily resulted to the film, and sometimes caused adjacent contacts to be shorted by the added indium rather than being connected only through the film.

To counter the problem of film damage and shorting of contacts, two razor-blade shields were manufactured, each with three 1 mm wide slots spaced about 5 mm apart (Fig. 4a). These shields provided three "legs" on both longitudinal sides of the film for instrumentation connections (Fig. 4b). Contact between external circuits and these legs could then easily be made utilizing the side tunnel and melted indium without destoying the main film or disturbing the current flow path at the pick-off point. With the shield, it was also possible to complete connections to the substrate and film after the vacuum deposit rather than before, without incurring damage to the main film. This method proved slightly more reliable, requiring less handling of the contact wires after their initial installation.

Specimens made, using both of the above methods, were found to be quite susceptible to loss of continuity between film and indium filler in cooling the specimen to liquid nitrogen temperature ($77^{o}K$) and then allowing it to return to room temperature ($\sim 20^{o}C$). Restoration of continuity with both melted indium and silver alloy paint was attempted with little permanent success. Continuity, established or re-established in this way at room temperature, would frequently be lost in cooling the specimen with liquid nitrogen as a test prior to immersion in liquid helium.

To overcome these difficulties, a piece of plexiglas with the same dimensions as that with the sample film was prepared as a holder for all leads, both power and instrumentation. Leads were passed through holes from the back of the holder, across its face, and then back through the holder. Insulation was removed on each lead only along that portion of its length that was across the face of the holder. The holder was

undercut or grooved slightly under each wire, these grooves thus serving to key each wire into correct position. The insulated ends of each wire were twisted together providing a flexible, but strong connection point.

This holder was then bolted to the specimen forming a "sandwich," and the "sandwich" bolted to the test assembly. The power leads were in contact with the main film, as were two of the instrumentation leads. These two instrumentation leads, both on the same side of, but near the ends of the main film, were used in determining the film's resistance. The additional instrumentation leads (three from each side) were in contact with the legs produced by the razor-blade mask. These leads were to be used for the Hall voltage measurement.

Although only one lead from each side was theoretically required for measuring the Hall voltage, physically obtaining perfect positioning of the leads opposite one another was highly unlikely. By having three leads from each side of the film, the possibility of obtaining a very close match was much better. While passing a current through the specimen, the dc microvolt-ammeter was used to measure the potential between opposite pairs of leads in order to find which set was closest to being at zero potential with no magnetic field applied.

For the first specimen tested in the holder, the leads from the middle legs were closest to being "balanced." Thus, these two middle legs plus one of the end legs were connected up as the Hall voltage measuring circuit (Fig. 3). Connecting the two leads from the same side across a variable resistor, provided a means of picking off the point that was electrically opposite the single pick-off point selected on the opposite side. Cooling the specimen with liquid nitrogen showed that a slight gradient was present in the film, necessitating a change from the

originally selected leads to another combination of two on one side and one on the other.

Testing with nitrogen prior to cooling with helium uncovered another difficulty apart from a small film gradient. Continuity obtained at room temperature, and subsequently lost at liquid nitrogen temperature would occasionally be regained at room temperature. Continuity obtained at room temperature and maintained at liquid nitrogen temperature would occasionally be lost upon again returning to room temperature. These phenomena, coupled with a random loosening of the sandwich clamping bolts, indicated the possibility of a temperature creep difference between the two pieces of plexiglas.

To compensate for this, more clamping bolts were used, all were firmly tightened and locking nuts were added. This action, although partially successful, resulted in the wires penetrating the film in several places and contact being lost after a cooling and warming cycle. These breaks in the film made re-establishing continuity difficult within the minimal movement constraints imposed on the wires by the holder and on the holder by the bolt holes.

To surmount this difficulty, small rectangular pads of indium were prepared from the wire used in production of the film by mashing flat small pieces of this wire. These pads were then inserted between film and the instrumentation lead wires and the sandwich rebolted snugly. Continuity was established and maintained over the entire temperature range. Upon completion of data taking, the specimen and holder were disassembled. A small area of film erosion was noted and attributed to water trapped between the two pieces of plexiglas as a result of condensation during one of the warming cycles. To dry the sample after a

continuity check with liquid nitrogen, a hot-air blower was employed to minimize the time period of film exposure to moisture.

Subsequent samples were prepared using the razor-blade mask, and pads were placed under each instrumentation lead contact wire upon initially bolting the sandwich together. No further problems in maintaining continuity were experienced. The pick-off points were standardized to be the two outside ones on one side and the middle one on the opposite side. Thus, if a slight gradient was present, as existed with the first sample, reconnecting would not be required. This, then, removed the necessity to have a check cooling in liquid nitrogen before setting up to take data, thus minimizing the possibility of creating an area of film erosion from entrapped condensation. All samples, after the second, were tested at room temperature for continuity before and after assembling into the sandwich. These samples were then installed into the experimental set-up and tested at nitrogen temperature by filling only the outer Dewar. All had continuity. Upon completion of data taking at liquid helium temperatures, the specimens were allowed to remain under vacuum until the system temperature had returned to ambient room conditions. Areas of film deterioration on these samples was minimal, indicating that water entrapment, encountered on the first two samples during continuity checkouts, was the probable cause of the erosion or film deterioration.

After consideration of the problems encountered and their solutions, it is felt that glass substrates, sandwiched between two pieces of plexiglas, one serving to hold the leads, the other as a mounting plate for the substrate, might prove to be quite satisfactory for future samples. Additionally, a shield or mask providing only two legs on one side of

the film, the midpoint between them being nearly across from a single leg on the opposite side, could be used, thus decreasing the spacing between the pick-off points from 10 mm to 5 mm or less, making possible a finer balancing of the variable connection against the fixed connection for measurement of the Hall voltage.

BIBLIOGRAPHY

1. E. H. Hall, Amer. J. Math. 2, 287 (1879).

2. J.-P. Jan, Solid State Physics Vol 5 (Academic Press Inc., New York, 1957), p. 40.

3. E. S. Borovik, Dokl. Akad. Nauk SSSR 75, 639 (1950).

4. E. S. Borovik and V. G. Volotskaya, Soviet Phys. - JETP 11, 189 (1960).

5. J. N. Cooper, P. Cotti, and F. B. Rasmussen, Phys. Ltrs. 19, 560 (1965).

6. W. van der Mark, J. L. Olsen, and F. B. Rasmussen, Intern. Conf. Low Temp. Phys. (1966).

7. E. H. Sondheimer, Phys. Rev. 80, 401 (1950).

8. A. C. Lauer and J. K. Nunnely, "Transition Time From Resistive to Superconducting State for Thin Indium Films" (Naval Postgraduate School Thesis, 1959), p. 4.

9. J. A. Eckert and R. G. Donnelly, "Temperature Dependence of Normal to Superconducting Transitions" (Naval Postgraduate School Thesis, 1960), p. 4.

10. J. L. Olsen, Electron Transport in Metals (Interscience Press, New York-London, 1962), p. 65.

11. L. Holland, Vacuum Deposition of Thin Films (Wiley, New York, 1956), p. 145.

12. W. Summer, Physical Laboratory Handbook (Van Nostrand, New York, 1966), p. 146.

13. C. R. MacDowell and F. P. Martin, "Effects of Silicon Monoxide Overlays on the Normal to Superconducting Transition Time in Thin Indium Films" (Naval Postgraduate School Thesis, 1963), p. 5.

14. G. L. Bower and K. R. Simila, "Normal to Superconducting Transition Times for Thin Films of Tin and Indium" (Naval Postgraduate School Thesis, 1964), p. 20.

INITIAL DISTRIBUTION LIST

		No. Copies
1.	Defense Documentation Center Cameron Station Alexandria, Virginia 22314	20
2.	Library Naval Postgraduate School Monterey, California 93940	2
3.	Chief of Naval Research Office of Naval Research Washington, D. C. 20360	1
4.	Commander Naval Ordnance Systems Command Headquarters Washington, D. C. 20360	1
5.	Professor John N. Cooper Department of Physics Naval Postgraduate School Monterey, California 93940	3
6.	LCDR Thomas E. Dyer, USN 1420 Via Marettimo Monterey, California 93940	1
7.	LCDR George Tsantes, Jr., USN Route No. 3, Box 336A Carmel, California 93921	1

DOCUMENT CONTROL DATA - R&D

(Security classification of title, body of abstract and indexing annotation must be entered when the overall report is classified)

1. ORIGINATING ACTIVITY *(Corporate author)*
Naval Postgraduate School
Monterey, California

2a. REPORT SECURITY CLASSIFICATION
Unclassified

2b. GROUP
NA

3. REPORT TITLE
The Hall Coefficient of Indium in Thin Evaporated Films

4. DESCRIPTIVE NOTES *(Type of report and inclusive dates)*
Thesis

5. AUTHOR(S) *(Last name, first name, initial)*
DYER, Thomas E., LCDR, USN
TSANTES, George (n), Jr., LCDR, USN

6. REPORT DATE	7a. TOTAL NO. OF PAGES	7b. NO. OF REFS
December 1967	71	14

8a. CONTRACT OR GRANT NO.	9a. ORIGINATOR'S REPORT NUMBER(S)
b. PROJECT NO. NA	NA
c.	9b. OTHER REPORT NO(S) *(Any other numbers that may be assigned this report)*
d.	None

10. AVAILABILITY/LIMITATION NOTICES
[redacted]

11. SUPPLEMENTARY NOTES	12. SPONSORING MILITARY ACTIVITY
None	Office of Naval Research

13. ABSTRACT

The Hall coefficient has been measured at liquid helium temperatures in the magnetic field range of 0.08-3.8 kilogauss for evaporated indium films with thicknesses between 900 and 2,500 Angstroms. For all films studied the Hall coefficient was positive; there was no sign reversal of the type observed in some rolled films at low magnetic fields. The coefficients obtained were slightly smaller than those previously reported for bulk films at comparable values of reduced magnetic field. Below the superconducting critical temperature in the weak-field region a large and unexpected transverse potential difference, independent of magnetic field direction, was observed. As the magnetic field was increased, this potential difference reversed sign and underwent damped, aperiodic oscillations in some samples. However, in the higher-field region a normal Hall voltage was present, and the Hall coefficient was in good agreement with the data above the critical temperature.

DD FORM 1 JAN 64 1473

14 KEY WORDS	LINK A		LINK B		LINK C	
	ROLE	WT	ROLE	WT	ROLE	WT
Hall Effect or Hall Coefficient						
Thin Evaporated Films						
Liquid Helium Temperatures						
Evaporated Indium Films						
Superconductive Indium Films						